Analytic and numerical study of preheating dynamics

D. Boyanovsky,[1] H. J. de Vega,[2] R. Holman,[3] and J. F. J. Salgado[2]
[1]*Department of Physics and Astronomy, University of Pittsburgh, Pittsburgh, Pennsylvania 15260*
[2]*Laboratoire de Physique Theorique et Hautes Energies, Université Pierre et Marie Curie (Paris VI) et Denis Diderot (Paris VII), Tour 16, 1er. étage, 4, Place Jussieu 75252 Paris, Cedex 05, France*
[3]*Department of Physics, Carnegie Mellon University, Pittsburgh, Pennsylvania 15213*
(Received 2 August 1996)

We analyze the phenomenon of preheating, i.e., explosive particle production due to parametric amplification of quantum fluctuations in the unbroken symmetry case, or spinodal instabilities in the broken symmetry phase, using the Minkowski space O(N) vector model in the large N limit to study the nonperturbative issues involved. We give analytic results for weak couplings and times short compared to the time at which the fluctuations become of the same order as the tree level terms, as well as numerical results including the full back reaction. In the case where the symmetry is unbroken, the analytical results agree spectacularly well with the numerical ones in their common domain of validity. In the broken symmetry case, interesting situations, corresponding to slow roll initial conditions from the unstable minimum at the origin, give rise to a new and unexpected phenomenon: the dynamical relaxation of the vacuum energy. That is, particles are abundantly produced at the expense of the quantum vacuum energy while the zero mode comes back to almost its initial value. In both cases we obtain analytically and numerically the equation of state which in both cases can be written in terms of an effective polytropic index that interpolates between vacuum and radiationlike domination. We find that simplified analyses based on the harmonic behavior of the zero mode, giving rise to a Mathieu equation for the nonzero modes, miss important physics. Furthermore, such analyses that do not include the full back reaction and do not conserve energy result in unbound particle production. Our results rule out the possibility of symmetry restoration by nonequilibrium fluctuations in the cases relevant for new inflationary scenarios. Finally, estimates of the reheating temperature are given, as well as a discussion of the inconsistency of a kinetic approach to thermalization when a nonperturbatively large number of particles are created. [S0556-2821(96)05524-5]

PACS number(s): 11.10.Wx, 11.15.Pg, 98.80.Cq

I. INTRODUCTION

It has recently been realized [1–3] that as the zero momentum mode of a quantum field evolves it can drive a large amplification of quantum fluctuations. This, in turn, gives rise to copious particle production for bosonic fields, creating quanta in a highly nonequilibrium distribution, radically changing the standard picture of reheating the postinflationary universe [4–6]. This process has other possible applications, such as in understanding the hadronization stage of the quark-gluon plasma [7] as well as trying to understand out-of-equilibrium particle production in strong electromagnetic fields and in heavy ion collisions [8–11].

The actual processes giving rise to preheating can be different depending on the potential for the scalar field involved as well as the initial conditions. For example, in new inflationary scenarios, where the inflaton field's zero mode evolves down the flat portion of a potential admitting spontaneous symmetry breaking, particle production occurs due to the existence of unstable field modes which get amplified until the zero mode leaves the instability region. These are the instabilities that give rise to spinodal decomposition and phase separation. In contrast, if we start with chaotic initial conditions, so that the field has large initial amplitude, particles are created from the parametric amplification of the quantum fluctuations due to the oscillations of the zero mode.

In this paper we analyze the details of this so-called *preheating* process both analytically as well as numerically. Preheating is a nonperturbative process, with typically $1/\lambda$ particles being produced, where λ is the self-coupling of the field. Because of this fact, any attempts at analyzing the detailed dynamics of preheating must also be nonperturbative in nature. This leads us to consider the O(N) vector model in the large N limit. This is a nonperturbative approximation that has many important features that justify its use: unlike the Hartree or mean-field approximation [3], it can be systematically improved in the $1/N$ expansion. It conserves energy, satisfies the Ward identities of the underlying symmetry, and again unlike the Hartree approximation it predicts the correct order of the transition in equilibrium.

This approximation has also been used in other nonequilibrium contexts [8–11]. In this work, we consider this model in Minkowski space, saving the discussion of the effects of the expansion of the universe for later work.

Our findings are summarized as follows.

We are able to provide consistent nonperturbative analytic estimates of the nonequilibrium processes occurring during the preheating stage taking into account the *exact* evolution of the inflaton zero mode for large amplitudes when the quantum back reaction due to the produced particles is negligible, i.e., at early and intermediate times. We also compute the momentum space distribution of the particle number as well as the effective equation of state during this stage. Ex-

plicit expressions for the growth of quantum fluctuations, the preheating time scale, as well as the effective (time-dependent) polytropic index defining the equation of state are given in Sec. III.

We then go beyond the early or intermediate time regime and evolve the equations of motion numerically, taking into account back-reaction effects. (That is, the nonlinear quantum field interaction.) These results confirm the analytic results in their domain of validity and show how, when back-reaction effects are large enough to compete with tree level effects, dissipational effects arise in the zero mode. Energy conservation is guaranteed in the full back-reaction problem, leading to the eventual shut off of particle production. This is an important ingredient in the dynamics that determines the relevant time scales.

We also find a novel dynamical relaxation of the vacuum energy in this regime when the theory is in the broken phase. Namely, particles are produced at the expense of the quantum vacuum energy while the zero mode contributes very little. We find a radiation type equation of state for late times ($p \approx \frac{1}{3}\varepsilon$) despite the lack of thermal equilibrium.

Finally we discuss the calculation of the reheating temperature in a class of models, paying particular attention to when the kinetic approach to thermalization and equilibration is applicable.

There have been a number of papers (see Refs. [1,12–15]) dedicated to the analysis of the preheating process where particle production and back-reaction are estimated in different approximations [16].

The layout of the paper is as follows. Section II presents the model, the evolution equations, the renormalization of the equations of motion, and introduces the relevant definitions of particle number, energy, and pressure and the details of their renormalization. The unbroken and broken symmetry cases are presented in detail and the differences in their treatment are clearly explained.

In Secs. III–V we present a detailed analytic and numerical treatment of both the unbroken and broken symmetry phases emphasizing the description of particle production, energy, pressure, and the equation of state. In the broken symmetry case, when the inflaton zero mode begins very close to the top of the potential, we find that there is a novel phenomenon of relaxation of the vacuum energy that explicitly shows where the energy used to produce the particles comes from. We also discuss why the phenomenon of symmetry restoration at preheating, discussed by various authors [1,13,17,18] is *not* seen to occur in the cases treated by us here and relevant for new inflationary scenarios [16].

In Sec. VI we provide estimates, under suitably specified assumptions, of the reheating temperature in the O(N) model as well as other models in which the inflaton couples to lighter scalars. In this section we argue that thermalization cannot be studied with a kinetic approach because of the nonperturbatively large occupation number of long-wavelength modes.

Finally, we summarize our results and discuss future avenues of study in the conclusions. We also include an appendix where we gather many important technical details on the evaluation of the Floquet mode functions and Floquet indices used in the main text.

II. SCALAR FIELD DYNAMICS IN THE LARGE N LIMIT

As mentioned above, preheating is a nonperturbative phenomenon so that a nonperturbative treatment of the field theory is necessary. This leads us to consider the O(N) vector model in the large N limit.

In this section we introduce this model, obtain the nonequilibrium evolution equations, the energy momentum tensor, and analyze the issue of renormalization. We will then be poised to study each particular case in detail in the later sections.

The Lagrangian density is

$$\mathcal{L}=\frac{1}{2}\partial_\mu\vec{\phi}\cdot\partial^\mu\vec{\phi}-V(\vec{\phi}\cdot\vec{\phi}),$$

$$V(\sigma,\vec{\pi})=\frac{1}{2}m^2\vec{\phi}\cdot\vec{\phi}+\frac{\lambda}{8N}(\vec{\phi}\cdot\vec{\phi})^2, \tag{2.1}$$

for λ fixed in the large N limit. Here $\vec{\phi}$ is an O(N) vector, $\vec{\phi}=(\sigma,\vec{\pi})$, and $\vec{\pi}$ represents the $N-1$ ''pions.'' In what follows, we will consider two different cases of the potential $V(\sigma,\vec{\pi})$, with ($m^2<0$) or without ($m^2>0$) symmetry breaking.

We can decompose the field σ into its zero mode and fluctuations $\chi(\vec{x},t)$ about the zero mode:

$$\sigma(\vec{x},t)=\sigma_0(t)+\chi(\vec{x},t). \tag{2.2}$$

The generating functional of real time nonequilibrium Green's functions can be written in terms of a path integral along a complex contour in time, corresponding to forward and backward time evolution and at finite temperature a branch down the imaginary time axis. This requires doubling the number of fields which now carry a label $\pm$ corresponding to forward ($+$), and backward ($-$) time evolution. The reader is referred to the literature for more details [19,20]. This generating functional along the complex contour requires the Lagrangian density along the contour, which for zero temperature is given by [3]

$$\begin{aligned}
&\mathcal{L}[\sigma_0+\chi^+,\vec{\pi}^+]-\mathcal{L}[\sigma_0+\chi^-,\vec{\pi}^-]\\
&\quad=\Bigg\{\mathcal{L}[\sigma_0,\vec{\pi}^+]+\frac{\delta\mathcal{L}}{\delta\sigma_0}\chi^+ +\frac{1}{2}(\partial_\mu\chi^+)^2+\frac{1}{2}(\partial_\mu\vec{\pi}^+)^2\\
&\qquad-\Bigg(\frac{1}{2!}V''(\sigma_0,\vec{\pi}^+)\chi^{+2}+\frac{1}{3!}V^{[3]}(\sigma_0,\vec{\pi}^+)(\chi^+)^3\\
&\qquad+\frac{1}{4!}V^{[4]}(\sigma_0,\vec{\pi}^+)(\chi^+)^4\Bigg)\Bigg\}\\
&\qquad-\{(\chi^+\to\chi^-),(\vec{\pi}^+\to\vec{\pi}^-)\}.
\end{aligned} \tag{2.3}$$

The tadpole condition $\langle\chi^\pm(\vec{x},t)\rangle=0$ will lead to the equations of motion as discussed in [3] and references therein.

A consistent and elegant version of the large N limit for nonequilibrium problems can be obtained by introducing an auxiliary field and is presented very thoroughly in Ref. [9]. This formulation has the advantage that it can incorporate the O($1/N$) corrections in a systematic fashion. Alternatively,

the large N limit can be implemented via a Hartree-like factorization [3] in which (i) there are no cross correlations between the pions and sigma field and (ii) the two point correlation functions of the pion field are diagonal in the $O(N-1)$ space of the remaining unbroken symmetry group. To leading order in large N both methods are completely equivalent and for simplicity of presentation we chose the factorization method.

The factorization of the nonlinear terms in the Lagrangian is (again for both $\pm$ components)

$$\chi^4 \to 6\langle\chi^2\rangle\chi^2 + \text{const}, \tag{2.4}$$

$$\chi^3 \to 3\langle\chi^2\rangle\chi, \tag{2.5}$$

$$(\vec{\pi}\cdot\vec{\pi})^2 \to 2\langle\vec{\pi}^2\rangle\vec{\pi}^2 - \langle\vec{\pi}^2\rangle^2 + O(1/N), \tag{2.6}$$

$$\vec{\pi}^2\chi^2 \to \langle\vec{\pi}^2\rangle\chi^2 + \vec{\pi}^2\langle\chi^2\rangle, \tag{2.7}$$

$$\vec{\pi}^2\chi \to \langle\vec{\pi}^2\rangle\chi, \tag{2.8}$$

To obtain a large N limit, we define

$$\vec{\pi}(\vec{x},t) = \psi(\vec{x},t)\overbrace{(1,1,\ldots,1)}^{N-1}\ ;\ \ \sigma_0(t) = \phi(t)\sqrt{N} \tag{2.9}$$

where the large N limit is implemented by the requirement that

$$\langle\psi^2\rangle = O(1), \quad \langle\chi^2\rangle = O(1), \quad \phi = O(1). \tag{2.10}$$

The leading contribution is obtained by neglecting the $O(1/N)$ terms in the formal large N limit. The resulting Lagrangian density is quadratic, with a linear term in χ:

$$\begin{aligned}\mathcal{L}[\sigma_0+\chi^+,\vec{\pi}^+] - \mathcal{L}[\sigma_0+\chi^-,\vec{\pi}^-] &= \{\tfrac{1}{2}(\partial_\mu\chi^+)^2 + \tfrac{1}{2}(\partial_\mu\vec{\pi}^+)^2 - \chi^+ V'(t) \\ &\quad - \tfrac{1}{2}\mathcal{M}_\chi^2(t)(\chi^+)^2 - \tfrac{1}{2}\mathcal{M}^2\vec{\pi}(t)(\vec{\pi}^+)^2\} \\ &\quad - \{(\chi^+\to\chi^-),(\vec{\pi}^+\to\vec{\pi}^-)\},\end{aligned} \tag{2.11}$$

where

$$V'(\phi(t),t) = \sqrt{N}\phi(t)\left[m^2 + \frac{\lambda}{2}\phi^2(t) + \frac{\lambda}{2}\langle\psi^2(t)\rangle\right], \tag{2.12}$$

$$\mathcal{M}^2\vec{\pi}(t) = m^2 + \frac{\lambda}{2}\phi^2(t) + \frac{\lambda}{2}\langle\psi^2(t)\rangle, \tag{2.13}$$

$$\mathcal{M}_\chi^2(t) = m^2 + \frac{3\lambda}{2}\phi^2(t) + \frac{\lambda}{2}\langle\psi^2(t)\rangle. \tag{2.14}$$

Note that we have used spatial translational invariance to write

$$\langle\psi^2(\vec{x},t)\rangle \equiv \langle\psi^2(t)\rangle. \tag{2.15}$$

The necessary (zero temperature) nonequilibrium Green's functions are constructed from the ingredients

$$G_k^>(t,t') = \frac{i}{2W_k}V_k(t)V_k^*(t'), \tag{2.16}$$

$$G_k^<(t,t') = \frac{i}{2W_k}V_k(t')V_k^*(t), \tag{2.17}$$

while the Heisenberg field operator $\psi(\vec{x},t)$ can be written as

$$\psi(\vec{x},t) = \frac{1}{\sqrt{\mathcal{V}}}\sum_k \frac{1}{\sqrt{2W_k}}[a_k V_k(t)e^{i\vec{k}\cdot\vec{x}} + a_k^\dagger V_k^*(t)e^{-i\vec{k}\cdot\vec{x}}], \tag{2.18}$$

where $a_k, a_k^\dagger$ are the canonical destruction and annihilation operators and $\mathcal{V}$ the quantization volume.

The evolution equations for the expectation value $\phi(t)$ and the mode functions $V_k(t)$ can be obtained by using the tadpole method [3] and are given by

$$\ddot{\phi}(t) + \phi(t)\left[m^2 + \frac{\lambda}{2}\phi^2(t) + \frac{\lambda}{2}\langle\psi^2(t)\rangle\right] = 0, \tag{2.19}$$

$$\left[\frac{d^2}{dt^2} + k^2 + m^2 + \frac{\lambda}{2}\phi^2(t) + \frac{\lambda}{2}\langle\psi^2(t)\rangle\right]V_k(t) = 0,$$

$$V_k(0) = 1, \quad \dot{V}_k(0) = -iW_k, \tag{2.20}$$

$$\langle\psi^2(t)\rangle = \int \frac{d^3k}{(2\pi)^3}\frac{|V_k(t)|^2}{2W_k}, \tag{2.21}$$

$$W_k = \sqrt{k^2 + m_0^2}. \tag{2.22}$$

The initial state $|i\rangle$ is chosen to be the vacuum for these modes, i.e., $a_k|i\rangle = 0$. The frequencies W_k (i.e., m_0^2) will determine the initial state and will be discussed for each particular case below.

The fluctuations $\chi(\vec{x},t)$ obey an independent equation, that does not enter in the dynamics of the evolution of the expectation value or the $\vec{\pi}$ fields to this order and decouples in the leading order in the large N limit [3].

It is clear from the above equations that the Ward identities of Goldstone's theorem are satisfied. Because $V'(\phi(t),t) = \sqrt{N}\phi(t)\mathcal{M}_{\vec{\pi}}^2(t)$, whenever $V'(\phi(t),t)$ vanishes for $\phi \neq 0$ then $\mathcal{M}_{\vec{\pi}}^2 = 0$ and the ''pions'' are the Goldstone bosons. This observation will be important in the discussions of symmetry breaking in a later section.

Since in this approximation the dynamics for the $\vec{\pi}$ and χ fields decouple, and the dynamics of χ does not influence that of ϕ, the mode functions or $\langle\psi^2\rangle$, we will only concentrate on the solution for the $\vec{\pi}$ fields. We note however, that if the dynamics is such that the asymptotic value of $\phi \neq 0$ the masses for χ and the ''pion'' multiplet $\vec{\pi}$ are different, and the original $O(N)$ symmetry is broken down to the $O(N-1)$ subgroup.

A. Renormalization of the O(N) model

We briefly review the most relevant features of the renormalization program in the large N limit that will be used frequently in our analysis. For more details the reader is referred to [9,3,11].

In this approximation, the Lagrangian is quadratic, and there are no counterterms. This implies that the equations for the mode functions must be finite. This requires that

$$m^2+\frac{\lambda}{2}\phi^2(t)+\frac{\lambda}{2}\langle\psi^2(t)\rangle=m_R^2+\frac{\lambda_R}{2}\phi^2(t)+\frac{\lambda_R}{2}\langle\psi^2(t)\rangle_R =-v(t). \tag{2.23}$$

Defining

$$\frac{V_k(t)}{\sqrt{W_k}}=\varphi_k(t),\quad \varphi_k(0)=\frac{1}{\sqrt{W_k}},\quad \dot{\varphi_k}(0)=-i\sqrt{W_k}, \tag{2.24}$$

the function $\varphi_k(t)$ is written as linear combinations of WKB solutions of the form

$$\varphi_k(t)=A_k\exp\left(\int_0^t R_k(t')dt'\right)+B_k\exp\left(\int_0^t R_k^*(t')dt'\right) \tag{2.25}$$

with $R_k(t)$ obeying a Riccati equation [11] and the coefficients A_k,B_k are fixed by the initial conditions. After some algebra we find

$$|\varphi_k(t)|^2\underset{k\to\infty}{\sim}\frac{1}{k}+\frac{v(t)}{2k^3}+\frac{3v(t)^2-\ddot{v}(t)}{8k^5}+O(k^{-7}) +\text{oscillatory terms},$$

$$|\dot{\varphi}_k(t)|^2\underset{k\to\infty}{\sim}k-\frac{v(t)}{2k}+\frac{\ddot{v}(t)-v(t)^2}{8k^3}+O(k^{-5}) +\text{oscillatory terms}. \tag{2.26}$$

Using this asymptotic form, we obtain [3,11] the renormalized quantities

$$m^2+\frac{\lambda}{16\pi^2}\left[\Lambda^2-m_R^2\ln\left(\frac{\Lambda}{\kappa}\right)\right]=m_R^2, \tag{2.27}$$

$$\lambda\left[1-\frac{\lambda_R}{16\pi^2}\ln\left(\frac{\Lambda}{\kappa}\right)\right]=\lambda_R, \tag{2.28}$$

and

$$\langle\psi^2(t)\rangle_R=\int\frac{k^2dk}{4\pi^2}\left\{|\varphi_k(t)|^2-\frac{1}{k}+\frac{\Theta(k-\kappa)}{2k^3} \times\left(m_R^2+\frac{\lambda_R}{2}\phi^2(t)+\frac{\lambda_R}{2}\langle\psi^2(t)\rangle_R\right)\right\}, \tag{2.29}$$

where we have introduced the (arbitrary) renormalization scale κ. Equations (2.23) and (2.29) lead to the renormalization conditions valid in the large N limit.

At this point it is convenient to absorb a further *finite* renormalization in the definition of the mass and introduce the quantities

$$M_R^2=m_R^2+\frac{\lambda_R}{2}\langle\psi^2(0)\rangle_R, \tag{2.30}$$

$$\tau=|M_R|t,\quad q=\frac{k}{|M_R|},\quad \Omega_q=\frac{W_k}{|M_R|}, \tag{2.31}$$

$$\eta^2(\tau)=\frac{\lambda_R}{2|M_R|^2}\phi^2(t), \tag{2.32}$$

$$g\Sigma(\tau)=\frac{\lambda_R}{2|M_R|^2}[\langle\psi^2(t)\rangle_R-\langle\psi^2(0)\rangle_R],\quad(\Sigma(0)=0), \tag{2.33}$$

$$g=\frac{\lambda_R}{8\pi^2}, \tag{2.34}$$

$$\varphi_q(\tau)\equiv|M_R|\varphi_k(t). \tag{2.35}$$

For simplicity in our numerical calculations later, we will choose the renormalization scale $\kappa=|M_R|$. The evolution equations are now written in terms of these dimensionless variables, in which overdots now stand for derivatives with respect to τ.

B. Unbroken symmetry

In this case $M_R^2=|M_R|^2$, and in terms of the dimensionless variables introduced above we find the equations of motion

$$\ddot{\eta}+\eta+\eta^3+g\eta(\tau)\Sigma(\tau)=0, \tag{2.36}$$

$$\left[\frac{d^2}{d\tau^2}+q^2+1+\eta(\tau)^2+g\Sigma(\tau)\right]\varphi_q(\tau)=0, \tag{2.37}$$

$$\varphi_q(0)=\frac{1}{\sqrt{\Omega_q}},\quad \dot{\varphi}_q(0)=-i\sqrt{\Omega_q}, \tag{2.38}$$

$$\eta(0)=\eta_0,\quad \dot{\eta}(0)=0. \tag{2.39}$$

As mentioned above, the choice of Ω_q determines the initial state. We will choose these such that at $t=0$ the quantum fluctuations are in the ground state of the oscillators at the initial time. Recalling that by definition $g\Sigma(0)=0$, we choose the dimensionless frequencies to be

$$\Omega_q=\sqrt{q^2+1+\eta_0^2}. \tag{2.40}$$

The Wronskian of two solutions of Eq. (2.37) is given by

$$\mathcal{W}[\varphi_q,\overline{\varphi_q}]=2i, \tag{2.41}$$

while $g\Sigma(\tau)$ is given by

$$g\Sigma(\tau)=g\int_0^\infty q^2dq\left\{|\varphi_q(\tau)|^2-\frac{1}{\Omega_q}+\frac{\theta(q-1)}{2q^3}[-\eta_0^2+\eta^2(\tau)+g\Sigma(\tau)]\right\}. \tag{2.42}$$

C. Broken symmetry

In the case of broken symmetry $M_R^2=-|M_R^2|$ and the field equations in the $N=\infty$ limit become

$$\ddot{\eta}-\eta+\eta^3+g\,\eta(\tau)\Sigma(\tau)=0, \tag{2.43}$$

$$\left[\frac{d^2}{d\tau^2}+q^2-1+\eta(\tau)^2+g\Sigma(\tau)\right]\varphi_q(\tau)=0, \tag{2.44}$$

where $\Sigma(\tau)$ is given in terms of the mode functions $\varphi_q(\tau)$ by the same expression of the previous case, Eq. (2.42). Now the choice of boundary conditions is more subtle. The situation of interest is when $0<\eta_0^2<1$, corresponding to the situation where the expectation value rolls down the potential hill from the origin. The modes with $q^2<1-\eta_0^2$ are unstable and thus do not represent simple harmonic oscillator quantum states. Therefore, one *must* choose a different set of boundary conditions for these modes. Our choice will be that corresponding to the ground state of an *upright* harmonic oscillator. This particular initial condition corresponds to a quench type of situation in which the initial state is evolved in time in an inverted parabolic potential (for early times $t>0$). Thus we shall use the following initial conditions for the mode functions:

$$\varphi_q(0)=\frac{1}{\sqrt{\Omega_q}},\quad \dot{\varphi}_q(0)=-i\sqrt{\Omega_q}, \tag{2.45}$$

$$\Omega_q=\sqrt{q^2+1+\eta_0^2}\ \text{ for }\ q^2<1-\eta_0^2, \tag{2.46}$$

$$\Omega_q=\sqrt{q^2-1+\eta_0^2}\ \text{ for }\ q^2>1-\eta_0^2,\quad 0\leqslant\eta_0^2<1, \tag{2.47}$$

along with the initial conditions for the zero mode given by Eq. (2.39).

D. Particle number

Although the notion of particle number is ambiguous in a time-dependent nonequilibrium situation, a suitable definition can be given with respect to some particular pointer state. We consider two particular definitions that are physically motivated and relevant as we will see later. The first is when we define particles with respect to the initial Fock vacuum state, while the second corresponds to defining particles with respect to the adiabatic vacuum state.

In the former case we write the spatial Fourier transform of the fluctuating field $\psi(\vec{x},t)$ in Eq. (2.9) and its canonical momentum $\Pi(\vec{x},t)$ as

$$\psi_k(t)=\frac{1}{\sqrt{2}}[a_k\varphi_k(t)+a^\dagger_{-k}\varphi^*_k(t)], \tag{2.48}$$

$$\Pi_k(t)=\frac{1}{\sqrt{2}}[a_k\dot{\varphi}_k(t)+a^\dagger_{-k}\dot{\varphi}^*_k(t)], \tag{2.49}$$

with the *time-independent* creation and annihilation operators, such that a_k annihilates the initial Fock vacuum state. Using the initial conditions on the mode functions, the Heisenberg field operators are written as

$$\psi_k(t)=\mathcal{U}^{-1}(t)\psi_k(0)\mathcal{U}(t)=\frac{1}{\sqrt{2W_k}}[\tilde{a}_k(t)+\tilde{a}^\dagger_{-k}(t)], \tag{2.50}$$

$$\Pi_k(t)=\mathcal{U}^{-1}(t)\Pi_k(0)\mathcal{U}(t)=-i\sqrt{\frac{W_k}{2}}[\tilde{a}_k(t)-\tilde{a}^\dagger_{-k}(t)], \tag{2.51}$$

$$\tilde{a}_k(t)=\mathcal{U}^{-1}(t)a_k\mathcal{U}(t), \tag{2.52}$$

with $\mathcal{U}(t)$ the time-evolution operator with the boundary condition $\mathcal{U}(0)=1$. The Heisenberg operators $\tilde{a}_k(t),\tilde{a}^\dagger_k(t)$ are related to $a_k,a_k^\dagger$ by a Bogoliubov (canonical) transformation (see Ref. [3] for details).

The particle number defined with respect to the initial Fock vacuum state is defined in term of the dimensionless variables introduced above as

$$N_q(\tau)=\langle\tilde{a}^\dagger_k(t)\tilde{a}_k(t)\rangle=\frac{\Omega_q}{4}\left[|\varphi_q(\tau)|^2+\frac{|\dot{\varphi}_q(\tau)|^2}{\Omega_q^2}\right]-\frac{1}{2}. \tag{2.53}$$

It is this definition of particle number that will be used for the numerical study.

In order to define the particle number with respect to the adiabatic vacuum state we note that the mode equations (2.37) and (2.44) are those of harmonic oscillators with time-dependent squared frequencies

$$\omega_q^2(\tau)=q^2\pm1+\eta^2(\tau)+g\Sigma(\tau) \tag{2.54}$$

with $+$ for the unbroken symmetry case and $-$ for the broken symmetry case, respectively. When the frequencies are real, the adiabatic modes can be introduced in the following manner:

$$\psi_k(t)=\frac{1}{\sqrt{2\omega_k(t)}}\alpha_k(t)\exp\left[-i\int_0^t\omega_k(t')dt'\right]+\alpha^\dagger_{-k}(t)\exp\left[i\int_0^t\omega_k(t')dt'\right], \tag{2.55}$$

$$\Pi_k(t)=-i\sqrt{\frac{\omega_k(t)}{2}}\left\{\alpha_k(t)\exp\left[-i\int_0^t\omega_k(t')dt'\right]-\alpha^\dagger_{-k}(t)\exp\left[i\int_0^t\omega_k(t')dt'\right]\right\}, \tag{2.56}$$

where now $\alpha_k(t)$ is a canonical operator that destroys the adiabatic vacuum state, and is related to $a_k,a_k^\dagger$ by a Bogoliubov transformation. This expansion diagonalizes the in-

stantaneous Hamiltonian in terms of the canonical operators $\alpha(t),\alpha^{\dagger}(t)$. The adiabatic particle number is

$$N_q^{ad}(\tau)=\langle\alpha_k^{\dagger}(t)\alpha_k(t)\rangle=\frac{\omega_q(\tau)}{4}\left[|\varphi_q(\tau)|^2+\frac{|\dot{\varphi}_q(\tau)|^2}{\omega_q^2(\tau)}\right]-\frac{1}{2}. \tag{2.57}$$

As mentioned above, the adiabatic particle number can *only* be defined when the frequencies $\omega_k(t)$ are real. Thus, in the broken symmetry state they can only be defined for wave vectors larger than the maximum unstable wave vector, $k>k_u=|M_R|\sqrt{1-\eta_0^2}$. These adiabatic modes and the corresponding adiabatic particle number have been used previously within the nonequilibrium context [8–10] and will be very useful in the analysis of the energy below. Both definitions coincide at $t=0$ because $\omega_q(0)=\Omega_q$. Notice that $N_q^{ad}(0)=N_q(0)=0$ due to the fact that we are choosing zero initial temperature. (We considered a nonzero initial temperature in Refs. [3,11]).

E. Energy and pressure

The energy momentum tensor for this theory is given by

$$T^{\mu\nu}=\partial^{\mu}\vec{\phi}\cdot\partial^{\nu}\vec{\phi}-g^{\mu\nu}[\partial_{\alpha}\vec{\phi}\cdot\partial^{\alpha}\vec{\phi}-V(\vec{\phi}\cdot\vec{\phi})]. \tag{2.58}$$

Using the large N factorization, Eqs. (2.4)–(2.7), (2.9) we find the energy density operator to be

$$\begin{aligned}\frac{E}{N\mathcal{V}}=&\frac{1}{2}\dot{\phi}^2(t)+\frac{1}{2}m^2\phi^2(t)+\frac{\lambda}{8}\phi^4(t)\\&+\frac{1}{2\mathcal{V}}\sum_k\left[\dot{\psi}_k(t)\dot{\psi}_{-k}(t)+\omega_k^2(t)\psi_k(t)\psi_{-k}(t)\right]\\&-\frac{\lambda}{8}\langle\psi^2(t)\rangle^2\\&+\text{linear terms in }\psi+O(1/N)\end{aligned} \tag{2.59}$$

$$\omega_k^2(t)=k^2+m^2+\frac{\lambda}{2}\phi^2(t)+\frac{\lambda}{2}\langle\psi^2(t)\rangle. \tag{2.60}$$

Taking the expectation value in the initial state and the infinite volume limit, defining $\varepsilon=\langle E\rangle/N\mathcal{V}$, and recalling that the tadpole condition requires that the expectation value of ψ vanishes, we find the expectation value of the energy to be

$$\begin{aligned}\varepsilon=&\frac{1}{2}\dot{\phi}^2(t)+\frac{1}{2}m^2\phi^2(t)+\frac{\lambda}{8}\phi^4(t)+\frac{1}{8\pi^2}\int k^2dk[|\dot{\varphi}_k(t)|^2\\&+\omega_k^2(t)|\varphi_k(t)|^2]-\frac{\lambda}{8}\langle\psi^2(t)\rangle^2.\end{aligned} \tag{2.61}$$

It is now straightforward to prove that this bare energy is conserved using the equations of motion (2.19)–(2.21). It is important to account for the last term when taking the time derivative because this term cancels a similar term in the time derivative of $\omega_k^2(t)$.

Since we consider translationally as well as rotationally invariant states, the expectation value of $T^{\mu\nu}$ takes the fluid form

$$T^{00}=\langle E\rangle,\quad T^{ij}=\langle P\rangle\delta^{ij},\quad T^{i0}=0. \tag{2.62}$$

We want to emphasize that the full evolution of the zero mode plus the back reaction with quantum fluctuations conserves energy. Such is obviously *not* the case in most treatments of reheating in the literature in which back reaction effects on the zero mode are neglected. Without energy conservation, the quantum fluctuations grow without bound. In cosmological scenarios energy is not conserved but its time dependence is not arbitrary; in a fixed space-time background metric it is determined by the covariant conservation of the energy momentum tensor. There again only a full account of the quantum back reaction will maintain covariant conservation of the energy momentum tensor.

We can write the integral in Eq. (2.61) as

$$\begin{aligned}\frac{1}{8\pi^2}\int_0^{\Lambda}k^2dk[|\dot{\varphi}_k(t)|^2+\omega_k^2(t)|\varphi_k(t)|^2]\\=\varepsilon_U+\frac{1}{2\pi^2}\int_{k_u}^{\Lambda}k^2dk\,\omega_k(t)\left(N_k^{ad}(t)+\frac{1}{2}\right),\end{aligned} \tag{2.63}$$

$$\varepsilon_U=\frac{1}{8\pi^2}\int_0^{k_u}k^2dk[|\dot{\varphi}_k(t)|^2+\omega_k^2(t)|\varphi_k(t)|^2], \tag{2.64}$$

where Λ is a spatial upper momentum cutoff, taken to infinity after renormalization. In the broken symmetry case, ε_U is the contribution to the energy momentum tensor from the unstable modes with negative squared frequencies, $k_u^2=|M_R|^2[1-\eta_0^2]$ and $N_k^{ad}(t)$ is the adiabatic particle number given by Eq. (2.57). For the unbroken symmetry case $\varepsilon_U=0$ and $k_u=0$.

This representation is particularly useful in dealing with renormalization of the energy. Since the energy is conserved, a subtraction at $t=0$ suffices to render it finite in terms of the renormalized coupling and mass. Using energy conservation and the renormalization conditions in the large N limit, we find that the contribution $\int_{k_u}^{\infty}k^2dk\,\omega_k(t)N_k^{ad}(t)$ is finite. This also follows from the asymptotic behaviors (2.26).

In terms of dimensionless quantities, the renormalized energy density is, after taking $\Lambda\to\infty$,

$$\begin{aligned}\varepsilon=&\frac{2|M_R|^4}{\lambda_R}\left\{\frac{\dot{\eta}^2}{2}+\frac{\eta^2}{2}\mathcal{M}^2(\tau)+\varepsilon_F-\frac{\mathcal{M}^4(\tau)}{4}\right.\\&\pm\frac{1}{2}\left(1-\frac{\lambda_R}{|M_R|^2}\langle\psi^2(0)\rangle_R\right)\mathcal{M}^2(\tau)+\frac{g}{8}\left[\frac{\mathcal{M}^4(\tau)}{4}\right.\\&+\mathcal{M}^2(\tau)q_u\sqrt{q_u^2+\mathcal{M}^2(\tau)}-2q_u[q_u^2+\mathcal{M}^2(\tau)]^{3/2}\\&\left.\left.+\mathcal{M}^4(\tau)\ln[q_u+\sqrt{q_u^2+\mathcal{M}^2(\tau)}]\right]\right\}+\mathcal{C},\end{aligned} \tag{2.65}$$

$$\begin{aligned}\varepsilon_F=&\frac{g}{2}\int_0^{q_u}q^2dq[|\dot{\varphi}_q|^2+\omega_q^2(\tau)|\varphi_q|^2]\\&+2g\int_{q_u}^{\infty}q^2dq\,\omega_q(\tau)N_q^{ad}(\tau),\end{aligned} \tag{2.66}$$

$$\mathcal{M}^2(\tau)=\pm 1+\eta^2(\tau)+g\Sigma(\tau), \quad \omega_q^2(\tau)=q^2+\mathcal{M}^2(\tau), \tag{2.67}$$

where the lower sign and $q_u=\sqrt{1-\eta_0^2}$ apply to the broken symmetry case while the upper sign and $q_u=0$ correspond to the unbroken symmetry case. The constant $\mathcal{C}$ is chosen such that ε coincides with the classical energy for the zero mode. The quantity $\mathcal{M}(\tau)$ is identified as the effective (dimensionless) mass for the ''pions.''

We find using the renormalized Eqs. (2.36), (2.37), (2.42), (2.42)–(2.44) that the renormalized energy ε is indeed *conserved* both for unbroken and for broken symmetry.

The pressure is obtained from the spatial components of the energy momentum tensor [see Eq. (2.62)] and we find the expectation value of the pressure density $p=\langle P\rangle/N\mathcal{V}$ to be given by

$$p=\dot{\phi}^2+\frac{1}{4\pi^2}\int k^2dk\left[|\dot{\varphi}_k(t)|^2+\frac{k^2}{3}|\varphi_k(t)|^2\right]-\varepsilon. \tag{2.68}$$

Using the large-k behavior of the mode functions (2.26), we find that aside from the time-independent divergence that is present also in the energy the pressure needs an extra subtraction $\frac{1}{6}\ddot{\phi}^2/k^3$ compared with the energy. Such a term corresponds to an additive renormalization of the energy-momentum tensor of the form

$$\delta T^{\mu\nu}=A(\eta^{\mu\nu}\partial^2-\partial^\mu\partial^\nu)\phi^2 \tag{2.69}$$

with A a (divergent) constant [21]. Performing the integrations with a spatial ultraviolet cutoff, and in terms of the renormalization scale κ introduced before, we find

$$A=-\frac{g}{12}\ln\left[\frac{\Lambda}{\kappa}\right]. \tag{2.70}$$

In terms of dimensionless quantities and after subtracting a time-independent quartic divergence, we finally find, setting $\Lambda=\infty$,

$$p=\frac{2|M_R|^4}{\lambda_R}\left\{\dot{\eta}^2+g\int_0^\infty q^2dq\left[\frac{q^2}{3}|\varphi_q(\tau)|^2+|\dot{\varphi}_q(\tau)|^2-\frac{4}{3}q-\frac{1}{3q}\mathcal{M}^2(\tau)+\frac{\theta(q-1)}{12q^3}\frac{d^2}{d\tau^2}[\eta^2+g\Sigma(\tau)]\right]\right\}-\varepsilon. \tag{2.71}$$

At this stage we can recognize why the effective potential is an irrelevant quantity to study the dynamics.

The sum of terms *without* ε_F in Eq. (2.65) for $q_u=0$ are identified with the effective potential in this approximation for a time-independent $\eta;g\Sigma$. These arise from the ''zero point'' energy of the oscillators with time-dependent frequency in Eq. (2.63).

In the broken symmetry case the term ε_F describes the dynamics of the spinodal instabilities [11] since the mode functions will grow in time. Ignoring these instabilities and setting $q_u=0$, as is done in a calculation of the effective potential, result in an imaginary part. In the unbroken symmetry ($q_u=0$) case the sum of terms without ε_F gives the effective potential in the large N limit, but the term ε_F describes the profuse particle production via parametric amplification, the mode functions in the unstable bands give a contribution to this term that eventually becomes nonperturbatively large and comparable to the tree level terms as will be described in detail below. Clearly, both in the broken and unbroken symmetry cases the effective potential misses *all* of the interesting nonperturbative dynamics, that is the exponential growth of quantum fluctuations and the ensuing particle production, either associated with unstable bands in the unbroken symmetry case or spinodal instabilities in the broken symmetry phase.

The expression for the renormalized energy density given by Eqs. (2.65)–(2.67) differs from the effective potential in several fundamental aspects: (i) it is always real as opposed to the effective potential that becomes complex in the spinodal region, (ii) it accounts for particle production and time-dependent phenomena.

The effective potential is a useless tool to study the dynamics precisely because it misses the profuse particle production associated with these dynamical, nonequilibrium and nonperturbative processes.

III. THE UNBROKEN SYMMETRY CASE

A. Analytic results

In this section we turn to the analytic treatment of Eqs. (2.36), (2.37), and (2.42) in the unbroken symmetry case. Our approximations will only be valid in the weak coupling regime and for times small enough so that the quantum fluctuations, i.e., $g\Sigma(\tau)$ are not large compared to the ''tree level'' quantities. We will see that this encompasses the times in which most of the interesting physics occurs.

Since $\Sigma(0)=0$, the back-reaction term $g\Sigma(\tau)$ is expected to be small for small g during an interval, say $0\leqslant\tau<\tau_1$. This time τ_1, to be determined below, determines the relevant time scale for preheating and will be called the preheating time.

During the interval of time in which the back-reaction term $g\Sigma(\tau)$ can be neglected, we can solve Eq. (2.36) in terms of elliptic functions, with the result

$$\eta(\tau)=\eta_0\,\mathrm{cn}(\tau\sqrt{1+\eta_0^2},k),$$

$$k=\frac{\eta_0}{\sqrt{2(1+\eta_0^2)}}, \tag{3.1}$$

where cn stands for the Jacobi cosine. Notice that $\eta(\tau)$ has period $4\omega\equiv 4K(k)/\sqrt{1+\eta_0^2}$, where $K(k)$ is the complete elliptic integral of first kind. In addition we note that since

$$\eta(\tau+2\omega)=-\eta(\tau), \tag{3.2}$$

if we neglect the back reaction in the mode equations, the ''potential'' $[-1-\eta^2(\tau)]$ is periodic with period 2ω. Inserting this form for $\eta(\tau)$ in Eq. (2.37) and neglecting $g\Sigma(\tau)$ yields

$$\left[\frac{d^2}{d\tau^2}+q^2+1+\eta_0^2-\eta_0^2\mathrm{sn}^2(\tau\sqrt{1+\eta_0^2},k)\right]\varphi_q(\tau)=0. \tag{3.3}$$

This is the Lamé equation for a particular value of the coefficients that makes it solvable in terms of Jacobi functions [22]. We summarize here the results for the mode functions. The derivations are given in the Appendix.

Since the coefficients of Eq. (3.3) are periodic with period 2ω, the mode functions can be chosen to be quasiperiodic (Floquet-type) with quasiperiod 2ω:

$$U_q(\tau+2\omega)=e^{iF(q)}U_q(\tau), \tag{3.4}$$

where the Floquet indices $F(q)$ are independent of τ. In the allowed zones, $F(q)$ is a real number and the functions are bounded with a constant maximum amplitude. In the forbidden zones $F(q)$ has a nonzero imaginary part and the amplitude of the solutions either grows or decreases exponentially.

Obviously, the Floquet modes $U_q(\tau)$ cannot obey in general the initial conditions given by Eq. (2.20) and the proper mode functions with these initial conditions will be obtained as linear combinations of the Floquet solutions. We normalize the Floquet solutions as

$$U_q(0)=1. \tag{3.5}$$

We choose $U_q(\tau)$ and $U_q(-\tau)$ as an independent set of solutions of the second order differential Eq. (3.3). It follows from Eq. (3.4) that $U_q(-\tau)$ has $-F(q)$ as its Floquet index.

We can now express the modes $\varphi_q(\tau)$ with the proper boundary conditions [see Eq. (2.20)] as the following linear combinations of $U_q(\tau)$ and $U_q(-\tau)$:

$$\varphi_q(\tau)=\frac{1}{2\sqrt{\Omega_q}}\left[\left(1-\frac{2i\Omega_q}{\mathcal{W}_q}\right)U_q(-\tau)+\left(1+\frac{2i\Omega_q}{\mathcal{W}_q}\right)U_q(\tau)\right], \tag{3.6}$$

where $\mathcal{W}_q$ is the Wronskian of the two Floquet solutions

$$\mathcal{W}_q\equiv W[U_q(\tau),U_q(-\tau)]=-2\dot{U}_q(0). \tag{3.7}$$

Equation (3.3) corresponds to a Schrödinger-like equation with a one-zone potential [23]. We find *two* allowed bands and *two* forbidden bands. The allowed bands correspond to

$$-1-\frac{\eta_0^2}{2}\leqslant q^2\leqslant 0 \quad\text{and}\quad \frac{\eta_0^2}{2}\leqslant q^2\leqslant+\infty, \tag{3.8}$$

and the forbidden bands to

$$-\infty\leqslant q^2\leqslant -1-\frac{\eta_0^2}{2} \quad\text{and}\quad 0\leqslant q^2\leqslant\frac{\eta_0^2}{2}. \tag{3.9}$$

The last forbidden band is for *positive* q^2 and hence will contribute to the exponential growth of the fluctuation function $\Sigma(\tau)$.

The mode functions can be written explicitly in terms of Jacobi ϑ functions for each band. We find, for the forbidden band,

$$U_q(\tau)=\exp[-\tau\sqrt{1+\eta_0^2}Z(2K(k)v)]\frac{\vartheta_4(0)\,\vartheta_1(v+\tau/2\omega)}{\vartheta_1(v)\,\vartheta_4(\tau/2\omega)}, \tag{3.10}$$

where v is a function of q in the forbidden band $0\leqslant q\leqslant\eta_0/\sqrt{2}$ defined by

$$q=\frac{\eta_0}{\sqrt{2}}\mathrm{cn}(2K(k)v,k), \quad 0\leqslant v\leqslant\frac{1}{2}, \tag{3.11}$$

and $Z(u)$ is the Jacobi zeta function [24]. It can be expanded in series as

$$2K(k)Z(2K(k)v)=4\pi\sum_{n=1}^{\infty}\frac{\hat{q}^n}{1-\hat{q}^{2n}}\sin(2n\pi v), \tag{3.12}$$

where $\hat{q}\equiv\exp[-\pi K'(k)/K(k)]$. The Jacobi ϑ functions can be expanded in series as [25]

$$\vartheta_1(v|\hat{q})=2\sum_{n=1}^{\infty}(-1)^{n+1}\hat{q}^{(n-1/2)^2}\sin(2n-1)\pi v,$$

$$\vartheta_4(v|\hat{q})=1+2\sum_{n=1}^{\infty}(-1)^n\hat{q}^{n^2}\cos(2n\pi v). \tag{3.13}$$

We explicitly see in Eq. (3.10) that $U_q(\tau)$ factorizes into a real exponential with an exponent linear in τ and an antiperiodic function of τ with period 2ω. Recall that

$$\vartheta_1(x+1)=-\vartheta_1(x), \quad \vartheta_4(x+1)=+\vartheta_4(x). \tag{3.14}$$

We see that the solution $U_q(\tau)$ decreases with τ. The other independent solution $U_q(-\tau)$ grows with τ.

The Floquet indices can be read comparing Eq. (3.4), (3.10), and (3.14),

$$F(q)=2iK(k)Z(2K(k)v)\pm\pi. \tag{3.15}$$

$U_q(\tau)$ turns out to be a real function in the forbidden band. It has real zeros at

$$\tau=2\omega(n-v), \quad n\in\mathcal{Z}, \tag{3.16}$$

and complex poles at

$$\tau=2\omega n_1+(2n_2+1)\omega', \quad n_1,n_2\in\mathcal{Z}, \tag{3.17}$$

where ω' is the complex period of the Jacobi functions. Notice that the pole positions are q independent, and that $U_q(\tau)$ becomes an antiperiodic function on the borders of this forbidden band, $q=0$ and $q=\eta_0/\sqrt{2}$. We find, using Eq. (3.10) and Ref. [24],

$$U_q(\tau)|_{q=0}=\mathrm{cn}(\tau\sqrt{1+\eta_0^2},k) \tag{3.18}$$

$$\lim_{q\to\,\eta_0/\sqrt{2}}[vU_q(\tau)]=\frac{1}{\pi\vartheta_3^2(0)}\mathrm{sn}(\tau\sqrt{1+\eta_0^2},k), \tag{3.19}$$

respectively.

The functions $U_q(\tau)$ transform under complex conjugation in the forbidden band as

$$[U_q(\tau)]^* = U_q(\tau). \tag{3.20}$$

For the allowed band $\eta_0/\sqrt{2} \leq q \leq \infty$, we find for the mode functions

$$U_q(\tau) = \exp\left[-\frac{\tau}{2\omega}\frac{\vartheta_1'}{\vartheta_1}\left(i\frac{K'(k)}{K(k)}v\right)\right] \times \frac{\vartheta_4(0)\,\vartheta_4\left(\frac{iK'(k)}{K(k)}v + \frac{\tau}{2\omega}\right)}{\vartheta_4\left(i\frac{K'(k)}{K(k)}v\right)\vartheta_4\left(\frac{\tau}{2\omega}\right)}, \tag{3.21}$$

where

$$q = \sqrt{\eta_0^2+1}\,\frac{\mathrm{dn}}{\mathrm{sn}}(2K'(k)v, k'), \tag{3.22}$$

$$0 \leq v \leq \frac{1}{2}, \quad \infty \geq q \geq \frac{\eta_0}{\sqrt{2}}. \tag{3.23}$$

We see that $U_q(\tau)$ in this allowed band factorizes into a phase proportional to τ and a complex periodic function with period 2ω. This function $U_q(\tau)$ has *no real zeros* in τ except when q is at the lower border $q = \eta_0/\sqrt{2}$. Its poles in τ are q independent and they are the same as those in the forbidden band [see Eq. (3.17)].

The Floquet indices can be read off by comparing Eqs. (3.4), (3.14), and (3.21),

$$F(q) = i\frac{\vartheta_1'}{\vartheta_1}\left(i\frac{K'(k)}{K(k)}v\right). \tag{3.24}$$

These indices are real in the allowed band.

The functions $U_q(\tau)$ transform under complex conjugation in the allowed band as

$$[U_q(\tau)]^* = U_q(-\tau). \tag{3.25}$$

Obviously these modes will give contributions to the fluctuation $\Sigma(\tau)$ which are always bounded in time and at long times will be subdominant with respect to the contributions of the modes in the forbidden band that grow exponentially.

The form of these functions is rather complicated, and it is useful to find convenient approximations of them for calculational convenience.

The expansion of the ϑ functions in powers of $\hat{q} = \exp[-\pi K'(k)/K(k)]$ converges quite rapidly in our case. Since $0 \leq k \leq 1/\sqrt{2}$ [see Eq. (3.1)], we have

$$0 \leq \hat{q} \leq e^{-\pi} = 0.0432139\ldots. \tag{3.26}$$

$\hat{q}$ can be computed with high precision from the series [25]

$$\hat{q} = \lambda + 2\lambda^5 + 15\lambda^9 + 150\lambda^{13} + 1707\lambda^{17} + \cdots,$$

where (not to be confused with the coupling constant)

$$\lambda \equiv \frac{1}{2}\,\frac{1-\sqrt{k'}}{1+\sqrt{k'}}. \tag{3.27}$$

We find from Eq. (3.1)

$$\lambda = \frac{1}{2}\,\frac{(1+\eta_0^2)^{1/4} - (1+\eta_0^2/2)^{1/4}}{(1+\eta_0^2)^{1/4} + (1+\eta_0^2/2)^{1/4}}. \tag{3.28}$$

The quantity λ can be computed and is a small number: for $0 \leq \eta_0 \leq \infty$, we find $0 \leq \lambda \leq 0.0432136\ldots$. Therefore, to very good approximation, with an error smaller than $\sim 10^{-7}$, we may use

$$\hat{q} = \frac{1}{2}\,\frac{(1+\eta_0^2)^{1/4} - (1+\eta_0^2/2)^{1/4}}{(1+\eta_0^2)^{1/4} + (1+\eta_0^2/2)^{1/4}}. \tag{3.29}$$

We find in the forbidden band from Eq. (3.10) and [24],

$$U_q(\tau) = \exp\{-4\tau\sqrt{1+\eta_0^2}\,\hat{q}\sin(2\pi v)[1 + 2\hat{q}(\cos 2\pi v - 2) + O(\hat{q}^2)]\}\frac{1-2\hat{q}}{1-2\hat{q}\cos\left(\frac{\pi\tau}{\omega}\right)}\,\frac{\sin\pi\left(v+\frac{\tau}{2\omega}\right)}{\sin\pi v} \times [1 + O(\hat{q}^2)], \tag{3.30}$$

where now we can relate v to q in the simpler form

$$q = \frac{\eta_0}{\sqrt{2}}\cos\pi v[1 - 4\hat{q}\sin^2\pi v + 4\hat{q}^2\sin^2\pi v(1 + 4\cos^2\pi v) + O(\hat{q}^3)], \tag{3.31}$$

which makes it more convenient to write $q(v)$ in the integrals, and

$$\frac{\pi}{2\omega} = \sqrt{1+\eta_0^2}[1 - 4\hat{q} + 12\hat{q}^2 + O(\hat{q}^4)], \tag{3.32}$$

where $0 \leq v \leq \frac{1}{2}$.

The Floquet indices can now be written in a very compact form amenable for analytical estimates

$$F(q) = 4i\pi\hat{q}\sin(2\pi v)[1 + 2\hat{q}\cos 2\pi v + O(\hat{q}^2)] + \pi. \tag{3.33}$$

In this approximation the zero mode (3.1) becomes

$$\eta(\tau) = \eta_0\cos\left(\frac{\pi\tau}{2\omega}\right)\left[1 - 4\hat{q}\sin^2\left(\frac{\pi\tau}{2\omega}\right) + O(\hat{q}^2)\right]. \tag{3.34}$$

This expression is very illuminating because we find that a Mathieu equation approximation, based on the first term of Eq. (3.34) to the evolution of the mode functions is *never* a good approximation. The reason for this is that the second and higher order terms are of the same order as the secular terms in the solution which after resummation lead to the identification of the unstable bands. In fact, whereas the Mathieu equation has *infinitely many* forbidden bands, the exact equation has only *one* forbidden band. Even for small $\hat{q}$, the Mathieu equation is not a good approximation to the Lamé equation [29].

From Eq. (3.21) analogous formulas can be obtained for the allowed band

$$U_q(\tau)=\exp\left\{-\frac{i\pi\tau}{2\omega}\coth\left[\frac{\pi K'(k)}{K(k)}v\right]\right\}\frac{1-2\hat{q}}{1-2\hat{q}\cos\left(\frac{\pi\tau}{\omega}\right)}$$

$$\times\frac{1-2\hat{q}\cos\left[\frac{\pi\tau}{\omega}-2iv\ln\hat{q}\right]}{1-2\hat{q}\cosh(2v\ln\hat{q})}[1+O(\hat{q}^2)], \quad (3.35)$$

where

$$q=\frac{\sqrt{\eta_0}}{2^{3/2}\sinh\left(\frac{\pi K'(k)}{K(k)}v\right)}\left(\frac{\eta_0^2+2}{\hat{q}}\right)^{1/4}\{1+2\hat{q}\cosh(2v\ln\hat{q})$$

$$+O(\hat{q}^2)\}. \quad (3.36)$$

Here,

$$0\leqslant v\leqslant\frac{1}{2}, \quad \infty\geqslant q\geqslant\frac{\eta_0}{\sqrt{2}}.$$

Note that Eq. (3.32) holds in all bands.

We can now estimate the size and growth of the quantum fluctuations, at least for relatively short times and weak couplings. For small times $0\leqslant\tau<\tau_1$ (to be determined consistently later) and small coupling $g\ll 1$, we can safely neglect the back-reaction term $g\Sigma(\tau)$ in Eq. (2.37) and express the modes $\varphi_q(\tau)$ in terms of the functions $U_q(\tau)$ and $U_q(-\tau)$; for this, however, we need the Wronskian, which in the forbidden band is found to be given by

$$\mathcal{W}_q=-\frac{1}{\omega}\frac{d}{dv}\ln\frac{\vartheta_1(v)}{\vartheta_4(v)}=-2\sqrt{1+\eta_0^2}\frac{\mathrm{cn}\,\mathrm{dn}}{\mathrm{sn}}(2vK(k),k). \quad (3.37)$$

In terms of the variable q^2 this becomes, after using Eq. (3.11),

$$\mathcal{W}_q=-2q\sqrt{\frac{\eta_0^2}{2}+1+q^2}\Big/\sqrt{\frac{\eta_0^2}{2}-q^2}. \quad (3.38)$$

This Wronskian is regular and nonzero except at the four borders of the bands.

We find from Eq. (3.6) that $|\varphi_q(\tau)|^2$ is given by

$$|\varphi_q(\tau)|^2=\frac{1}{4\Omega_q}\left\{[U_q(\tau)+U_q(-\tau)]^2+\frac{4\Omega_q^2}{\mathcal{W}_q^2}[U_q(\tau)-U_q(-\tau)]^2\right\}, \quad (3.39)$$

where we took into account Eqs. (3.20) and (3.25). Notice that both terms in the (RHS) of Eq. (3.39) are real and positive for real q. For very weak coupling and after renormalization, the contribution to $g\Sigma(\tau)$ from the stable bands will always be perturbatively small, while the contribution from the modes in the unstable band will grow exponentially in time eventually yielding a nonperturbatively large contribution. Thus these are the only important modes for the fluctuations and the back reaction. An estimate of the preheating time scale can be obtained by looking for the time when $g\Sigma(\tau)$ is of the same order of the classical contributions to the equations of motion. In order to obtain an estimate for the latter, we consider the average over a period of the classical zero mode:

$$1+\langle\eta^2(\tau)\rangle=(1+\eta_0^2)\left[\frac{2E(k)}{K(k)}-1\right] \quad (3.40)$$

which yields for small and large initial amplitudes the results

$$\langle\eta^2(\tau)\rangle\underset{\eta_0\to 0}{\sim}\frac{\eta_0^2}{2}, \quad (3.41)$$

$$\langle\eta^2(\tau)\rangle\underset{\eta_0\to\infty}{\sim}0.4569\ldots\eta_0^2. \quad (3.42)$$

Therefore the average over a period of $\eta^2(\tau)$ is to a very good approximation $\eta_0^2/2$ for all initial amplitudes. This result provides an estimate for the preheating time scale τ_1; this occurs when $g\Sigma(\tau_1)\approx(1+\eta_0^2/2)$. Furthermore, at long times [but before $g\Sigma\approx(1+\eta_0^2/2)$] we need only keep the exponentially growing modes and $g\Sigma(\tau)$ can be approximated by

$$g\Sigma_{\mathrm{est}}(\tau)=\frac{g}{4}\int_0^{\eta_0/\sqrt{2}}q^2dq\,\frac{1}{\Omega_q}\left[1+\frac{4\Omega_q^2}{\mathcal{W}_q^2}\right]|U_q(-\tau)|^2. \quad (3.43)$$

Moreover, choosing τ such that the oscillatory factors in $U_q(-\tau)$ attain the value 1 (the envelope), and using Eq. (3.10) we finally obtain:

$$\Sigma_{\mathrm{est\text{-}env}}(\tau)=\frac{1}{4}\int_0^{\eta_0/\sqrt{2}}q^2dq\,\frac{1}{\Omega_q}\left[1+\frac{4\Omega_q^2}{\mathcal{W}_q^2}\right]\times\exp[2\tau\sqrt{1+\eta_0^2}Z(2K(k)v,k)], \quad (3.44)$$

where v depends on the integration variable through Eq. (3.11).

The Jacobi Z function can be accurately represented using Eq. (3.12)

$$Z(2K(k)v,k)=4\hat{q}\sin 2\pi v[1-2\hat{q}(2-\cos 2\pi v)]+O(\hat{q}^3), \quad (3.45)$$

where we recall that $\hat{q}<0.0433$.

The integral (3.44) will be dominated by the point q that maximizes the coefficient of τ in the exponent. This happens at $q=q_1, v=v_1$, where

$$q_1=\tfrac{1}{2}\,\eta_0(1-\hat{q})+O(\hat{q}^2), \quad (3.46)$$

$$Z(2K(k)v_1,k)=4\hat{q}(1-4\hat{q})+O(\hat{q}^3). \quad (3.47)$$

We can compute the integral (3.44) by saddle point approximation to find

TABLE I. Quantum fluctuations $\Sigma(\tau)\approx 1/N\sqrt{\tau}e^{B\tau}$ during the preheating period.

η_0	$\hat{q}$	B	N
1	0.017972387 . . .	0.1887167 . . .	3.778 . . .
3	0.037295557 . . .	0.8027561 . . .	0.623 . . .
4	0.03966577 . . .	1.1007794 . . .	0.4 . . .
$\eta_0\to\infty$	0.043213918 . . .	$0.28595318\,\eta_0+O(\eta_0^{-1})$	$3.147\,\eta_0^{-3/2}[1+O(\eta_0^{-2})]$

$$\Sigma_{\text{est-env}}(\tau)=\frac{q_1^2\left[1+\frac{4\Omega_{q_1}^2}{\mathcal{W}_{q_1}^2}\right]}{2\Omega_{q_1}}\exp[8\,\tau\sqrt{1+\eta_0^2}\hat{q}(1-4\hat{q})]$$
$$\times\int_{-\infty}^{\infty}dq\exp[-64\tau(q-q_1)^2\hat{q}\sqrt{1+\eta_0^2}\eta_0^{-2}$$
$$\times(1-2\hat{q})][1+O(\hat{q})]$$
$$=\frac{\eta_0^3\sqrt{\pi}\left[1+\frac{4\Omega_{q_1}^2}{\mathcal{W}_{q_1}^2}\right]}{64(1+\eta_0^2)^{1/4}\sqrt{\tau\hat{q}}\Omega_{q_1}}\exp[8\,\tau\sqrt{1+\eta_0^2}\hat{q}$$
$$\times(1-4\hat{q})]\left[1+O\left(\frac{1}{\tau}\right)\right]. \tag{3.48}$$

We can relate $\hat{q}$ to η_0 using Eq. (3.29), and we have used the small $\hat{q}$ expansion

$$Z''(2K(k)v_1,k)=-16\hat{q}(1-4\hat{q})+O(\hat{q}^3), \tag{3.49}$$

$$\left.\frac{dq}{dv}\right|_{v_1}=-\frac{1}{2\pi}(1-9\hat{q})+O(\hat{q}^2). \tag{3.50}$$

In summary, during the preheating time where parametric resonance is important, $\Sigma_{\text{est-env}}(\tau)$ can be represented to a very good approximation by the formula

$$\Sigma_{\text{est-env}}(\tau)=\frac{1}{N\sqrt{\tau}}\,e^{B\tau}, \tag{3.51}$$

where B and N are functions of η_0 given by

$$B=8\,\sqrt{1+\eta_0^2}\hat{q}(1-4\hat{q})+O(\hat{q}^3),$$

$$N=\frac{64}{\pi^{1/2}}\,\frac{(1+\eta_0^2)^{1/4}\sqrt{\hat{q}}\Omega_{q_1}}{\eta_0^3\left[1+\frac{4\Omega_{q_1}^2}{\mathcal{W}_{q_1}^2}\right]}$$
$$=\frac{4}{\sqrt{\pi}}\sqrt{\hat{q}}\frac{(4+3\,\eta_0^2)\sqrt{4+5\,\eta_0^2}}{\eta_0^3(1+\eta_0^2)^{3/4}}[1+O(\hat{q})], \tag{3.52}$$

and Eq. (3.29) gives $\hat{q}$ as a function of η_0. This is one of the main results of this work.

We display in Table I some relevant values of $\hat{q}, B$, and N as functions of η_0.

We notice that the limiting values of B and N for $\eta_0\to\infty$ yield a very good approximation even for $\eta_0\sim 1$. Namely,

$$\Sigma(\tau)\approx\sqrt{\frac{\eta_0^3}{\tau}}\frac{e^{B_\infty\eta_0\tau}}{N_\infty}, \tag{3.53}$$

with the asymptotic values given by

$$B_\infty=8e^{-\pi}(1-4e^{-\pi})[1+O(\eta_0^{-2})]$$
$$=0.285953\ldots[1+O(\eta_0^{-2})], \tag{3.54}$$

$$N_\infty=\frac{12}{\sqrt{\pi}}\sqrt{5}e^{-\pi/2}[1+O(\eta_0^{-2})]=3.147\ldots[1+O(\eta_0^{-2})]. \tag{3.55}$$

These rather simple expressions (3.51)–(3.55) allow us to perform analytic estimates with great accuracy and constitute one of our main analytic results. The accuracy of this result will be discussed below in connection with the full numerical analysis including back reaction.

Using this estimate for the back-reaction term, we can now estimate the value of the preheating time scale τ_1 at which the back reaction becomes comparable to the classical terms in the differential equations. Such a time is defined by $g\Sigma(\tau_1)\sim(1+\eta_0^2/2)$. From the results presented above, we find

$$\tau_1\approx\frac{1}{B}\ln\frac{N(1+\eta_0^2/2)}{g\sqrt{B}}. \tag{3.56}$$

The time interval from $\tau=0$ to $\tau\sim\tau_1$ is when most of the particle production takes place. After $\tau\sim\tau_1$ the quantum fluctuation becomes large enough to shutoff the growth of the modes and particle production essentially stops. We will compare these results to our numerical analysis below.

We can now use our analytic results to study the different contributions to the energy and pressure coming from the zero mode and the quantum fluctuations and begin by analyzing the contribution to the energy ϵ_0 and pressure p_0 from the zero mode $\eta(\tau)$.

The dimensionless energy and pressure (normalized by the factor $2M_R^4/\lambda_R$) are given by the expressions

$$\epsilon_0(\tau)=\tfrac{1}{2}[\,\dot{\eta}^2+\eta(\tau)^2+\tfrac{1}{2}\,\eta(\tau)^4],$$

$$p_0(\tau)=\tfrac{1}{2}[\,\dot{\eta}^2-\eta(\tau)^2-\tfrac{1}{2}\,\eta(\tau)^4]. \tag{3.57}$$

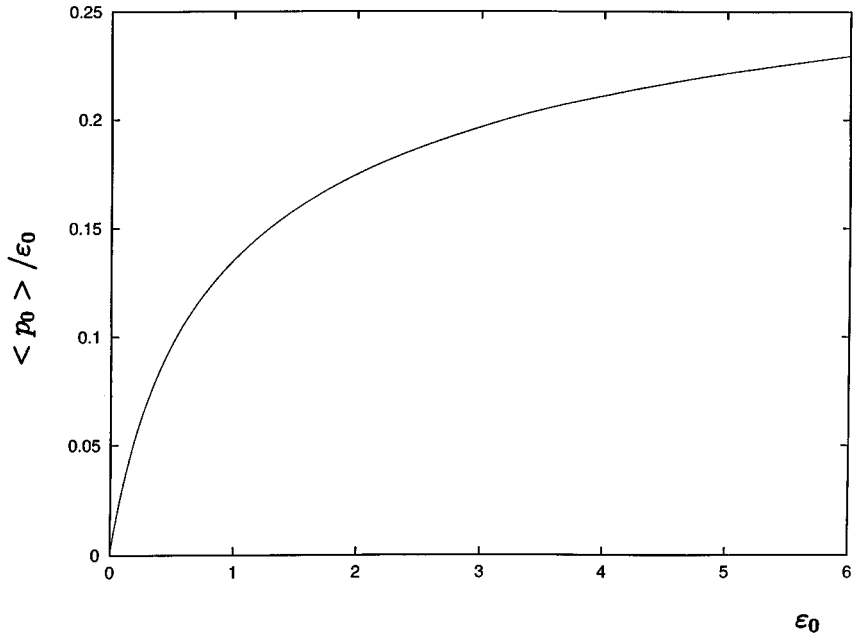

FIG. 1. The ratio $\langle p_0\rangle/\varepsilon_0$ for zero mode vs $\lambda_R\varepsilon_0/2|M_R|^4$ for the unbroken symmetry case.

When the back-reaction term $g\Sigma(\tau)$ can be neglected, we can use Eq. (3.1) as a good approximation to $\eta(\tau)$. In this approximation,

$$\epsilon_0=\tfrac{1}{2}\,\eta_0^2[1+\tfrac{1}{2}\,\eta_0^2],$$

$$p_0(\tau)+\epsilon_0=\eta_0^2(1+\eta_0^2)\,\mathrm{sn}^2\,\mathrm{dn}^2(\tau\sqrt{1+\eta_0^2},k). \quad (3.58)$$

The zero mode energy is conserved and the pressure oscillates between plus and minus ϵ_0 with period 2ω.

Averaging $p_0(\tau)$ over one period yields

$$\langle p_0\rangle\equiv\frac{1}{2\omega}\int_0^{2\omega}d\tau p_0(\tau). \quad (3.59)$$

Inserting Eq. (3.58) into Eq. (3.59) yields [26]

$$\langle p_0\rangle=-\frac{1}{6}\,\eta_0^2\left[1-\frac{1}{2}\,\eta_0^2\right]+\frac{2}{3}(1+\eta_0^2)\left[1-\frac{E(k)}{K(k)}\right], \quad (3.60)$$

where k is given by Eq. (3.1).

$\langle p_0\rangle$ vanishes for small η_0 faster than ϵ_0,

$$\langle p_0\rangle\underset{\eta_0\to 0}{\sim}\tfrac{1}{24}\,\eta_0^4+O(\eta_0^6), \quad (3.61)$$

so that the zero mode contribution to the equation of state is that of dust for small η_0. For large η_0 we find from Eq. (3.60),

$$\langle p_0\rangle\underset{\eta_0\to\infty}{\sim}\frac{1}{12}\,\eta_0^4+\eta_0^2\left[\frac{1}{2}-\frac{2}{3}\,\frac{E(1/\sqrt{2})}{K(1/\sqrt{2})}\right]+O(1), \quad (3.62)$$

where $\frac{1}{2}-\frac{2}{3}E(1/\sqrt{2})/K(1/\sqrt{2})=0.01437\ldots$. The equation of state approaches that of radiation for $\eta_0\to\infty$:

$$\langle p_0\rangle\underset{\eta_0\to\infty}{\sim}\epsilon_0\left[\frac{1}{3}-\frac{0.6092\ldots}{\eta_0^2}+O(\eta_0^{-4})\right]. \quad (3.63)$$

Thus, we see that for small amplitudes the zero-mode stress energy, averaged over an oscillation period, behaves as dust while for large amplitudes, the behavior is that of a radiation fluid. The ratio $<p_0>/\varepsilon_0$ for zero mode vs ε_0 is shown in Fig. 1.

The contribution from the $k\neq 0$ modes originates in the quantum fluctuations during the the stage of parametric amplification.

Since we have fluid behavior, we can define an effective (time-dependent) polytropic index $\gamma(\tau)$ as

$$\gamma(\tau)\equiv\frac{p(\tau)}{\varepsilon}+1, \quad (3.64)$$

where renormalized quantities are understood throughout. Within a cosmological setting whenever $\gamma(\tau)$ reaches a constant value, such equation of state implies a scale factor $R(\tau)=R_0\tau^{2/3\gamma}$.

In the case being studied here, that of Minkowski space, ε is time independent and hence equal to the initial energy density (divided by N and restoring prefactors) which after a suitable choice of the constant C is given by

$$\varepsilon=\frac{2|M_R|^4}{\lambda_R}\left\{\frac{1}{2}\,\eta_0^2\left[1+\frac{1}{2}\,\eta_0^2\right]\right\}. \quad (3.65)$$

As argued before, for weak coupling the important contribution to the quantum fluctuations comes from the modes in unstable bands, since these grow exponentially in time and give rise to a nonperturbatively large contribution. Thus, we concentrate only on these modes in calculating the pressure.

The contribution of the forbidden band to the renormalized $p(\tau)+\varepsilon$ can be written as

$$[p(\tau)+\varepsilon]_{\rm unst}=\frac{2|M_R|^4}{\lambda_R}\left\{g\int_0^{\eta_0/\sqrt{2}}q^2dq\left[|\dot{\varphi}_q(\tau)|^2+\frac{1}{3}q^2|\varphi_q(\tau)|^2\right]\right\}. \tag{3.66}$$

After renormalization, the terms that we have neglected in this approximation are perturbatively small (of order g) whereas the terms inside the brackets eventually become of order 1 (comparable to the tree level contribution). We now only keep the exponentially growing pieces in the mode functions $\varphi_q(\tau)$ and $\dot{\varphi}_q(\tau)$ since these will dominate the contribution to the pressure. This is simplified considerably by writing, to leading order in $\hat{q}$,

$$\dot{\varphi}_q(\tau)=\varphi_q(\tau)\left\{\sqrt{1+\eta_0^2}\cot\left[\pi\left(\upsilon-\frac{\tau}{2\omega}\right)\right]+O(\hat{q})\right\}. \tag{3.67}$$

Averaging over a period of oscillation yields

$$[p(\tau)+\varepsilon]_{\rm unst}=\frac{2|M_R|^4}{\lambda_R}\left\{\frac{g}{4}\int_0^{\eta_0/\sqrt{2}}\frac{q^2dq}{(4\pi)^2}\times\frac{1}{2\Omega_q\sin^2\pi\upsilon}\left[1+\frac{4\Omega_q^2}{\mathcal{W}_q^2}\right] \tag{3.68}$$

$$\times\exp[2\tau\sqrt{1+\eta_0^2}Z(2K(k)\upsilon,k)]\times\left[1+\eta_0^2+\frac{1}{3}q^2\right]\Bigg\}. \tag{3.69}$$

This integral is similar to the one in Eq. (3.44) and we find that they are proportional in the saddle point approximation. In fact,

$$[p(\tau)+\varepsilon]_{\rm unst}=\frac{2|M_R|^4}{\lambda_R}\left[g\Sigma_{\text{est-env}}(\tau)\left(1+\frac{13}{12}\eta_0^2\right)\right], \tag{3.70}$$

where $\Sigma_{\text{est-env}}(\tau)$ is given by Eq. (3.51).

The effective polytropic index $\gamma(\tau)$ is:

$$\gamma(\tau)=g\Sigma_{\text{est-env}}(\tau)\frac{12+13\eta_0^2}{3\eta_0^2(\eta_0^2+2)}. \tag{3.71}$$

When $g\Sigma_{\text{est-env}}(\tau_1)\sim 1+\eta_0^2/2$, i.e., at the end of the preheating phase, $\gamma(\tau)$ is given by

$$\gamma_{\rm eff}\propto\frac{12+13\eta_0^2}{6\eta_0^2}. \tag{3.72}$$

We note here that for very large η_0 the effective polytropic index is $\gamma_{\rm eff}\simeq 13/6\sim O(1)$. It is clear then that the physics can be interpreted in terms of two fluids, one the contribution from the zero mode and the other from the fluctuations, each with an equation of state that is neither that of dust nor of radiation, but described in terms of an effective polytropic index.

We can now use our approximations to obtain an estimate for the number of particles produced during the preheating stage. In terms of dimensionless quantities, the particle number, defined with respect to the initial Fock vacuum state, is given by Eq. (2.53).

This particle number will only obtain a significant contribution from the unstable modes in the forbidden band where to leading order in $\hat{q}$ we can approximate $\varphi_q(\tau)$ and $\dot{\varphi}_q(\tau)$ by its exponentially growing pieces [see Eq. (3.39)], as

$$|\varphi_q(\tau)|^2\simeq\frac{1}{4\,\Omega_q}\left[1+\frac{4\Omega_q^2}{\mathcal{W}_q^2}\right]|U_q(-\tau)|^2, \tag{3.73}$$

$$|\dot{\varphi}_q(\tau)|^2\simeq(1+\eta_0^2)\cot^2\left[\pi\left(\upsilon-\frac{\tau}{2\omega}\right)\right]|\varphi_q(\tau)|^2+O(\hat{q}). \tag{3.74}$$

The total number of produced particles $N(\tau)$ per volume $|M_R|^3$ is given by

$$\mathcal{N}=\frac{N(\tau)}{|M_R|^3}\equiv\int\frac{d^3q}{(2\pi)^3}N_q(\tau). \tag{3.75}$$

The asymptotic behavior (2.26) ensures that this integral converges.

Following the same steps as in Eqs. (3.44) and (3.68), we find

$$N(\tau)_{\rm unst}=\frac{1}{8\pi^2}\Sigma_{\text{est-env}}(\tau)\left[\frac{1+\eta_0^2}{\Omega_{q_1}}+\Omega_{q_1}\right]=\frac{1}{\lambda_R}\frac{4+\frac{9}{2}\eta_0^2}{\sqrt{4+5\eta_0^2}}[g\Sigma_{\text{est-env}}(\tau)], \tag{3.76}$$

where we used Eq. (3.46) and $\Sigma_{\text{est-env}}(\tau)$ is given by the simple formula (3.51). Notice that by the end of the preheating stage, when $g\Sigma(\tau)\approx 1+\eta_0^2/2$ the total number of particles produced is nonperturbatively large, both in the amplitude as well as in the coupling

$$\mathcal{N}_{\rm tot}\approx\frac{1}{\lambda_R}\frac{(4+\frac{9}{2}\eta_0^2)(1+\eta_0^2/2)}{\sqrt{4+5\eta_0^2}}. \tag{3.77}$$

The total number of *adiabatic* particles can also be computed in a similar manner with a very similar result insofar as the nonperturbative form in terms of coupling and initial amplitude.

B. Numerical results

We now evolve our equations for the zero and nonzero modes numerically, including the effects of back reaction. We will see that up to the preheating time, our analytic results agree extremely well with the full numerical evolution.

The procedure used was to solve Eqs. (2.36) and (2.37) with the initial conditions (2.38)–(2.40) and (2.42) using a fourth order Runge-Kutta algorithm for the differential equation and an 11-point Newton-Cotes integrator to compute the fluctuation integrals. We tested the cutoff sensitivity by running our code for cutoffs $\Lambda/|M_R|=100,70,50,20$ and for very small couplings (which is the case of interest). We

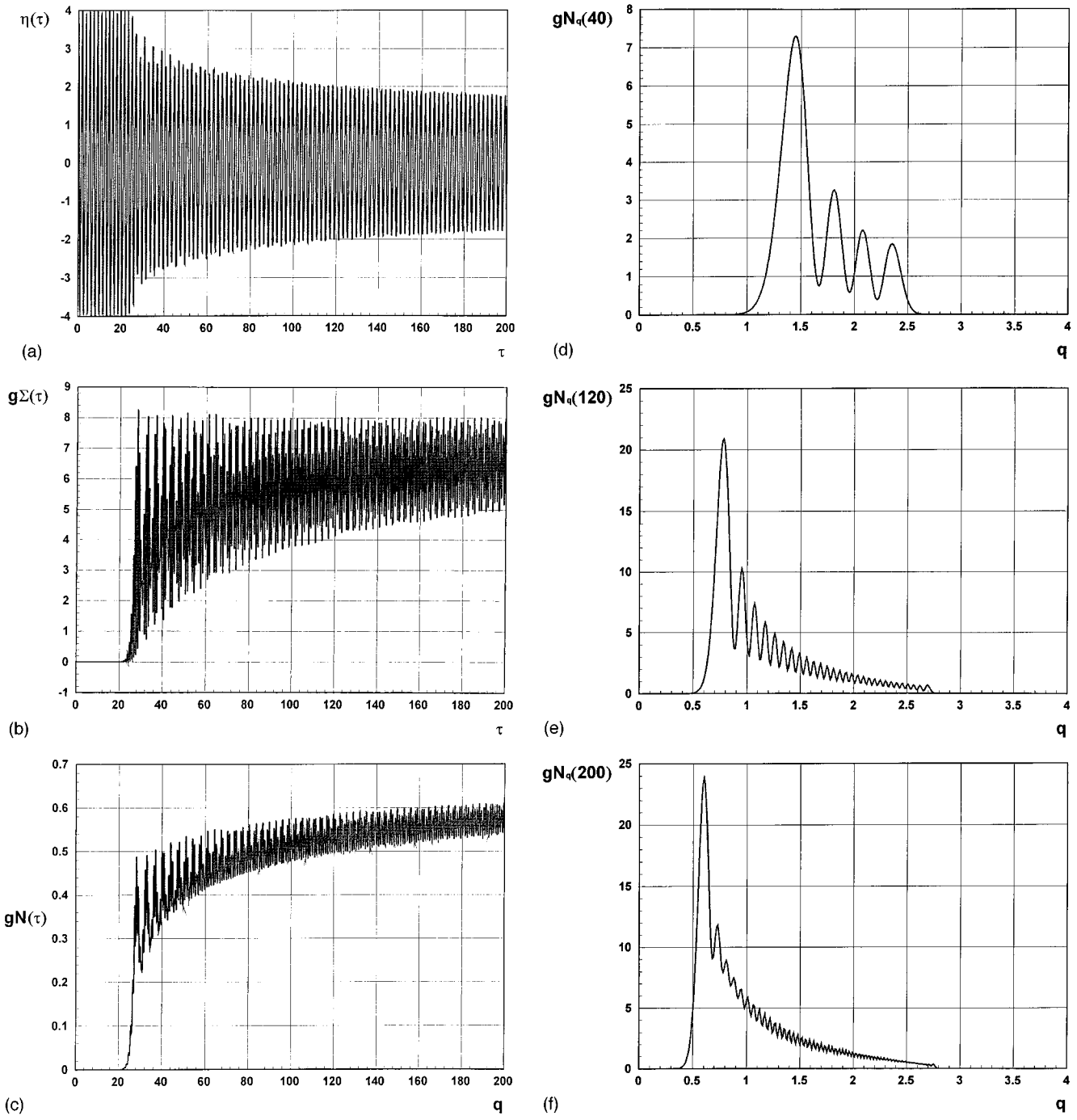

FIG. 2. (a) $\eta(\tau)$ vs τ for the unbroken symmetry case with $\eta_0=4$, $g=10^{-12}$. (b) $g\Sigma(\tau)$ for the same values of the parameters as in (a). The agreement with the analytic prediction is to within 5% for $0<\tau\leqslant 30$. (c) $g\mathcal{N}(\tau)$ for the same parameters as in (a). (d) $gN_q(\tau)$ vs q for $\tau=40$ for the same values of parameters as in (a). (e) $gN_q(\tau)$ vs. q for $\tau=120$ for the same values of parameters as in (a). (f) $gN_q(\tau)$ vs q for $\tau=200$ for the same values of parameters as in (a). (g) $(\lambda_R/2|M_R|^4)p(\tau)$ for the same values of the parameters as in (a). (h) Asymptotically the average over a period gives $p_\infty\approx\varepsilon/3$.

found no appreciable cutoff dependence. The typical numerical error both in the differential equations and the integrals is less than one part in 10^9.

Figure 2(a) shows $\eta(\tau)$ vs τ for $\eta_0=4.0$, $g=10^{-12}$. For this weak coupling, the effect of back reaction is negligible for a long time, allowing several undamped oscillations of the zero mode. Figure 2(b) shows $g\Sigma(\tau)$ vs τ. It can be seen that the back reaction becomes important when $g\Sigma(\tau)\approx 1+\eta_0^2/2$ as the evolution of $\eta(\tau)$ begins to damp out. This happens for $\tau\approx 25$, in excellent agreement with the analytic prediction given by Eq. (3.56) $\tau_1=26.2\ldots$, the difference between the analytic estimate for $\Sigma(\tau)$ given by Eq. (3.53) and the numerical result is less than 5% in the range $0<\tau<30$. Figure 2(c) shows $g\mathcal{N}(\tau)$ vs τ and we see that the analytic expression (3.77) gives an approximate estimation $\lambda_R\mathcal{N}_{tot}\approx 74.6\ldots$ for the final number of produced particles.

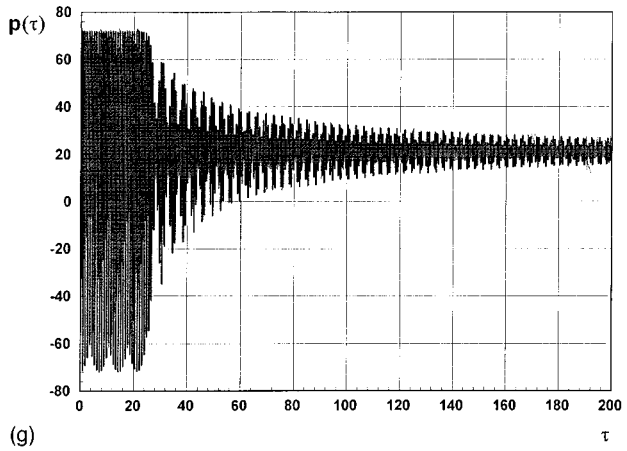

FIG. 2 (*Continued*).

Figures 2(d)–2(f), show $gN_q(\tau)$ for $\tau=40,120,200$; we see that the prediction of the width of the unstable band $0<q<\eta_0/\sqrt{2}$ is excellent and is valid even for very long times beyond the regime of validity of the small time, weak coupling approximation. However, we see that the peak becomes higher, narrower and moves towards $q\approx 0.5$ as time evolves beyond τ_1. This feature persists in all numerical studies of the unbroken phase that we have carried out; these changes in the peak width, height, and position are clearly a result of back-reaction effects. We have searched for unstable bands for $0<q<20$ and we only found one band precisely in the region predicted by the analytic estimate. All throughout the evolution *there is only one unstable band*. The band develops some structure with the height, position, and width of the peak varying at long times but no other unstable bands develop and the width of the band remains constant. For values of q outside the unstable band we find typically $gN_q<10^{-13}$ at all times. This is a remarkable and unexpected feature.

Obviously, this is very different from the band structure of a Mathieu equation. The Mathieu equation gives rise to an infinite number of narrowing bands, so that quantitative estimates of particle production, etc. using the Mathieu equation approximation would be gross misrepresentations of the actual dynamics, with discrepancies that are nonperturbatively large when the back reaction becomes important [16]. Since particle production essentially happens in the forbidden bands, the quantitative predictions obtained from a single forbbiden band and an infinite number, as predicted by WKB or Mathieu equation analysis, will yield different physics.

We have carried the numerical evolution including only the wave vectors in the unstable region and we find that this region of q wave vectors is the most relevant for the numerics. Even using a cutoff as low as $q_c=4$ in this case gives results that are numerically indistinguishable from those obtained with much larger cutoffs $q_c=70$–100. The occupation number of modes outside the unstable bands very quickly becomes negligibly small and for $q\approx 4$ it is already of the same order of magnitude as the numerical error $\leqslant 10^{-10}$. Clearly, this is a feature of the weak coupling case under consideration. Keeping only the contribution of the modes in the unstable band, the energy and pressure can be written as

$$\varepsilon=\frac{2|M_R|^4}{\lambda_R}\left\{\frac{\dot{\eta}^2}{2}+\frac{\eta^2}{2}+\frac{\eta^4}{4}+2g\int_0^{q_c}q^2dq\Omega_q N_q(\tau)+\frac{g}{2}\Sigma(\tau)\left[\eta^2(\tau)-\eta_0^2+\frac{g}{2}\Sigma(\tau)\right]+O(g)\right\}, \tag{3.78}$$

$$p=\frac{2|M_R|^4}{\lambda_R}\left\{g\int_0^{q_c}q^2dq\left[\frac{q^2}{3}|\varphi_q(\tau)|^2+|\dot{\varphi}(\tau)|^2\right]+\dot{\eta}^2+O(g)\right\}-\varepsilon, \tag{3.79}$$

$$q_c=\frac{\eta_0}{\sqrt{2}}, \tag{3.80}$$

where we have made explicit that we have neglected terms of order g in Eqs. (3.78)–(3.79). The terms multiplied by g in Eqs. (3.78) and (3.79) become of order 1 during the preheating stage. For the parameters used in Figs. 2, we have checked numerically that the energy (3.78) is conserved to order g within our numerical error. Figure 2(g) shows the pressure $2|M_R|^4p(\tau)/\lambda_R$ vs τ. Initially, $p(0)=-\varepsilon$ (vacuum dominated) but at the end of preheating the equation of state becomes almost that of radiation $p_\infty=\varepsilon/3$.

For very small coupling ($g\sim 10^{-12}$), the back reaction shuts off suddenly the particle production at the end of the preheating [see Fig. 2(c)]. Later on (τ larger than 100 for $g\sim 10^{-12}$), the time evolution is periodic in a very good approximation. That is, this nonlinear system exhibits a limiting cycle behavior. The modulus of the k modes does not grow in time and no particle production takes place. This tells us that no forbidden bands are present for $q^2>0$ in the late time regime.

We have numerically studied several different values of η_0, g finding the same qualitative behavior for the evolution of the zero mode, particle production, and pressure. In all cases we have found remarkable agreement (at most 5% difference) with the analytical predictions in the time regime for which $0<g\Sigma(\tau)\leqslant 1$. The asymptotic value of the pressure, however, only becomes consistent with a radiation dominated case for large initial amplitudes. For smaller amplitudes $\eta_0=1$ we find that asymptotically the polytropic index is smaller than 4/3. This asymptotic behavior is beyond the regime of validity of the approximations in the analytic treatment and must be studied numerically. This polytropic index depends crucially on the band structure because most of the contribution comes from the unstable modes.

IV. THE BROKEN SYMMETRY CASE

A. Analytic results

As in the unbroken case, for $g\ll 1$ we can neglect $g\Sigma(\tau)$ in Eq. (2.43) until a time τ_2 at which point the fluctuations have grown to be comparable to the 'tree level' terms.

We then find, for $0\leqslant\eta_0\leqslant 1$,

$$\eta(\tau)=\frac{\eta_0}{\mathrm{dn}\left(\tau\sqrt{1-\frac{\eta_0^2}{2}},k\right)},$$

$$k=\sqrt{\frac{1-\eta_0^2}{1-\frac{\eta_0^2}{2}}}. \tag{4.1}$$

Notice that $\eta(\tau)$ has period $2\omega\equiv 2K(k)/\sqrt{1-\eta_0^2/2}$. The elliptic modulus k is given by Eq. (4.1).

For $1\leq\eta_0\leq\sqrt{2}$ we find

$$\eta(\tau)=\eta_0\,\mathrm{dn}(\tau\eta_0/\sqrt{2},k),$$

$$k=\sqrt{2(1-\eta_0{}^{-2})}. \tag{4.2}$$

This solution follows by shifting Eq. (4.1) by a half-period and changing $\eta_0^2\to 2-\eta_0^2$. It has a period $2\omega\equiv 2\sqrt{2}/\eta_0 K(k)$. For $\eta_0\to 1$, $2\omega\to\pi\sqrt{2}$ and the oscillation amplitude vanishes, since $\eta=1$ is a minimum of the classical potential.

For $\eta_0>\sqrt{2}$ we obtain

$$\eta(\tau)=\eta_0\,\mathrm{cn}(\sqrt{\eta_0^2-1}\,\tau,k),$$

$$k=\frac{\eta_0}{\sqrt{2(\eta_0{}^2-1)}}. \tag{4.3}$$

This solution has $4\omega\equiv 4K(k)/\sqrt{\eta_0^2-1}$ as period.

The solutions for $\eta_0<\sqrt{2}$ and $\eta_0>\sqrt{2}$ are qualitatively different since in the second case $\eta(\tau)$ oscillates over the two minima $\eta=\pm 1$. In the limiting case $\eta_0=\sqrt{2}$ these solutions degenerate into the instanton solution

$$\eta(\tau)=\frac{\sqrt{2}}{\cosh\tau}, \tag{4.4}$$

and the period becomes infinite.

Inserting this form for $\eta(\tau)$ in Eq. (2.44) and neglecting $g\Sigma(\tau)$ yields, for $0\leq\eta_0\leq 1$,

$$\left[\frac{d^2}{d\tau^2}+q^2-1+\frac{\eta_0^2}{\mathrm{dn}^2\left(\tau\sqrt{1-\frac{\eta_0^2}{2}},k\right)}\right]\varphi_q(\tau)=0. \tag{4.5}$$

This is again a Lamé equation for a one-zone potential and can also be solved in closed form in terms of Jacobi functions. We summarize here the results for the mode functions, with the derivations again given in the Appendix.

As for unbroken symmetry case, there are *two* allowed bands and *two* forbidden bands. The allowed bands for $0\leq\eta_0\leq 1$ correspond to

$$0\leq q^2\leq\frac{\eta_0^2}{2}\ \text{ and }\ 1-\frac{\eta_0^2}{2}\leq q^2\leq+\infty, \tag{4.6}$$

and the forbidden bands to

$$-\infty\leq q^2\leq 0\ \text{ and }\ \frac{\eta_0^2}{2}\leq q^2\leq 1-\frac{\eta_0^2}{2}. \tag{4.7}$$

The last forbidden band exists for positive q^2 and hence contributes to the growth of $\Sigma(\tau)$.

The Floquet solutions obey Eqs. (3.4) and (3.5) and the modes $\varphi_q(\tau)$ can be expressed in terms of $U_q(\tau)$ and $U_q(-\tau)$ following Eq. (3.6).

It is useful to write the solution $U_q(\tau)$ in terms of Jacobi ϑ functions. For the forbidden band $\eta_0^2/2\leq q^2\leq 1-\eta_0^2/2$ after some calculation (see the Appendix),

$$U_q(\tau)=\exp[-\tau\sqrt{1-\eta_0^2/2}\,Z(2K(k)v)]\frac{\vartheta_3(0)\,\vartheta_2\left(v+\frac{\tau}{2\omega}\right)}{\vartheta_2(v)\,\vartheta_3\left(\frac{\tau}{2\omega}\right)}, \tag{4.8}$$

where $0\leq v\leq\frac{1}{2}$ is related with q through

$$q^2=1-\frac{\eta_0^2}{2}-(1-\eta_0^2)\,\mathrm{sn}^2(2K(k)v,k), \tag{4.9}$$

and k is a function of η_0 as defined by Eq. (4.1).

We see explicitly here that $U_q(\tau)$ factorizes into a real exponential with an exponent linear in τ and an antiperiodic function of τ with period 2ω.

The Floquet indices for this forbidden band are given by

$$F(q)=2iK(k)Z(2K(k)v)\pm\pi. \tag{4.10}$$

For the allowed band $1-\eta_0^2/2\leq q^2\leq+\infty$, we find for the modes,

$$U_q(\tau)=\exp\left[-(\tau/2\omega)\,\vartheta_1'/\vartheta_1\left(\frac{i\alpha}{2\omega}\right)\right]\frac{\vartheta_3(0)\,\vartheta_3\left(\frac{i\alpha+\tau}{2\omega}\right)}{\vartheta_3\left(\frac{i\alpha}{2\omega}\right)\vartheta_3\left(\frac{\tau}{2\omega}\right)}, \tag{4.11}$$

where q and α are related by

$$q=\frac{\sqrt{1-\frac{\eta_0^2}{2}}}{\mathrm{sn}\left(\alpha\sqrt{1-\frac{\eta_0^2}{2}},k'\right)},$$

with $K'(k)/\sqrt{1-\eta_0^2}\geq\alpha\geq 0$. The Floquet indices for this first allowed band are given by

$$F(q)=i\frac{\vartheta_1'}{\vartheta_1}\left(\frac{i\alpha}{2\omega}\right). \tag{4.12}$$

Analogous expressions hold in the other allowed band, $0\leq q^2\leq\eta_0^2/2$:

$$U_q(\tau)=\exp\left[-(\tau/2\omega)\,\vartheta_2'/\vartheta_2\left(\frac{i\alpha}{2\omega}\right)\right]\frac{\vartheta_3(0)\,\vartheta_4\left(\frac{i\alpha+\tau}{2\omega}\right)}{\vartheta_4\left(\frac{i\alpha}{2\omega}\right)\vartheta_3\left(\frac{\tau}{2\omega}\right)}. \tag{4.13}$$

Here, $q=\eta_0/\sqrt{2};\mathrm{sn}(\alpha\sqrt{1-\eta_0^2/2},k')$ and $K'(k)/\sqrt{1-\eta_0^2}\geqslant\alpha\geqslant 0$, and the Floquet indices for this band are given by

$$F(q)=i\frac{\vartheta_2'}{\vartheta_2}\left(\frac{i\alpha}{2\omega}\right). \tag{4.14}$$

For $\eta_0\approx 1$ the situation is very similar to the unbroken symmetry case; the zero mode oscillates quasiperiodically around the minimum of the tree level potential. There are effects from the curvature of the potential, but the dynamics can be analyzed in the same manner as in the unbroken case, with similar conclusions and will not be repeated here.

The case $\eta_0\ll 1$ is especially interesting [3] for broken symmetry because of new and interesting phenomena [3] that have been recently associated with symmetry restoration [1,13,17,18].

In this limit, the elliptic modulus k [see Eq. (4.1)] approaches unity and the (real) period 2ω grows as

$$2\,\omega\simeq 2K(k)+O(\eta_0^2)\simeq 2\,\ln\left(\frac{\sqrt{32}}{\eta_0}\right)+O(\eta_0^2). \tag{4.15}$$

In this limit, both the potential in Eq. (4.5) and the mode function (4.8) can be approximated by hyperbolic functions [24]:

$$\frac{1}{\mathrm{dn}\left(\tau\sqrt{1-\frac{\eta_0^2}{2}},k\right)}=\cosh\tau+O(\eta_0^2), \tag{4.16}$$

$$Z(u)=\tanh u-\frac{u}{\Lambda}+O(\eta_0^2), \tag{4.17}$$

where

$$\cosh u=\frac{4}{\eta_0^2}\left(q-\sqrt{q^2-\frac{\eta_0^2}{2}}\right)[1+O(\eta_0^2)],$$

$$\Lambda\equiv\ln\left(\frac{\sqrt{32}}{\eta_0}\right),$$

$$0\leqslant u\leqslant\Lambda. \tag{4.18}$$

Using the imaginary Jacobi transformation [24],

$$\vartheta_{2,3}(v|\hat{q})=\sqrt{\frac{K(k)}{K(k')}}\,\exp\{-[\pi K(k)/K(k')]v^2\}\times\vartheta_{4,3}\left(-i\frac{K(k)}{K(k')}v\,\middle|\,\dot{q}\right), \tag{4.19}$$

where $\hat{q}=e^{-\pi K(k')/K(k)}$, $\dot{q}=e^{-\pi K(k)/K(k')}$, and the series expansions [24]

$$\vartheta_3(v|\hat{q})=1+2\sum_{n=1}^{\infty}\hat{q}^{n^2}\cos(2\pi n v), \tag{4.20}$$

$$\vartheta_4(v|\hat{q})=\vartheta_3(v+\tfrac{1}{2}|\hat{q}), \tag{4.21}$$

we can derive expressions for the mode functions $U_q(\tau)$ valid for small η_0:

$$U_q(\tau)=\exp[-\tau\tanh u(1+\eta_0^2/8)]\times\frac{1-\frac{\eta_0^2}{8}\cosh u\cosh(u+2\tau)}{1-\frac{\eta_0^2}{8}\cosh u}[1+O(\eta_0^2)]. \tag{4.22}$$

Here u is related with q through Eq. (4.18). We see that the function $U_q(-\tau)$ grows with τ almost as e^{τ} for q near the lower border of the forbidden band $u\simeq\Lambda$. This fast growth can be interpreted as the joint effect of the nonperiodic exponential factor in Eq. (4.8) and the growth of the periodic ϑ functions. Since the real period is here of the order Λ, the two effects cannot be separated. The unstable growth for $\tau\leqslant\omega$ also reflects the spinodal instabilities associated with phase separation [11].

In this case, there is a range of parameters for which the quantum fluctuations grow to become comparable to the tree level contribution within just one or very few periods. The expression (4.22) determines that $\Sigma(\tau)\approx e^{2\tau}$ from the contributions of modes near the lower edge of the band. The condition for the quantum fluctuations to become of order 1 within just one period of the elliptic function is $ge^{4\omega}\approx 1$ which leads to the conclusion that for $\eta(0)<g^{1/4}$; the quantum fluctuations grow very large before the zero mode can actually execute a single oscillation. In such a situation an analysis in terms of Floquet (quasiperiodic) solutions is not correct because the back reaction prevents the zero mode from oscillating enough times for periodicity to be a reasonable approximation.

We now analyze the behavior of the pressure for the zero mode to compare to the previous case. In the approximation where Eqs. (4.1)–(4.3) hold and adjusting the constant $\mathcal{C}$ in the definition of the energy, we have

$$\epsilon_0=\tfrac{1}{4}(\eta_0^2-1)^2,$$

$$p_0(\tau)=-\epsilon_0+\dot{\eta}(\tau)^2. \tag{4.23}$$

Inserting Eqs. (4.1)–(4.3) in Eq. (4.23) yields

$$0\leqslant\eta_0\leqslant 1:\quad p_0(\tau)=-\epsilon_0\left[1-8\,\mathrm{sn}^2\mathrm{cn}^2\times\left((\tau+K)\sqrt{1-\frac{\eta_0^2}{2}},k\right)\right],$$

$$1\leqslant\eta_0\leqslant\sqrt{2}:\quad p_0(\tau)=-\epsilon_0[1-8\,\mathrm{sn}^2\mathrm{cn}^2(\tau\eta_0/\sqrt{2},k)],$$

$$\eta_0\geqslant\sqrt{2}:\quad p_0(\tau)=-\epsilon_0[1-8k^2\mathrm{sn}^2\mathrm{dn}^2(\tau\sqrt{\eta_0^2-1},k)]. \tag{4.24}$$

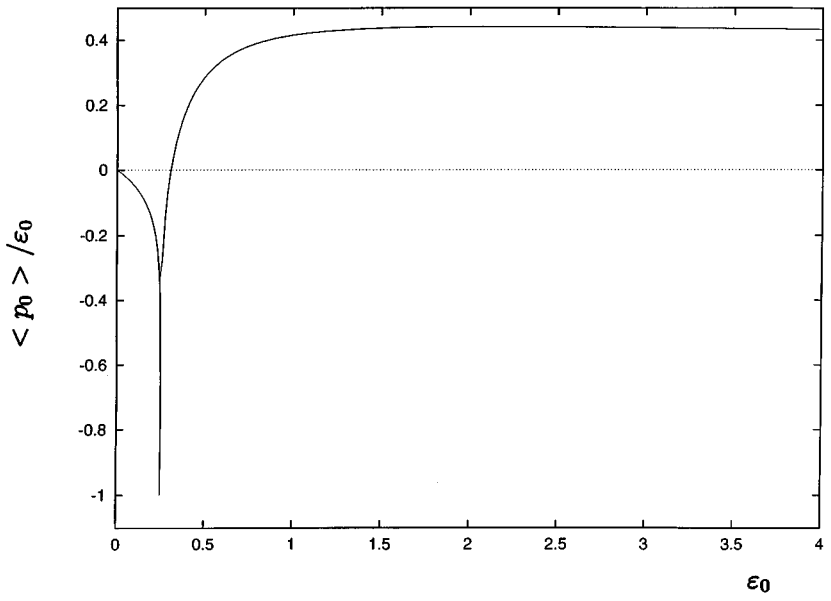

FIG. 3. The ratio $\langle p_0\rangle/\varepsilon_0$ for zero mode vs $\lambda_R\varepsilon_0/2|M_R|^4$ for the broken symmetry case.

Notice that the functional form of the elliptic modulus k as a function of η_0 is different in each interval [see Eqs. (4.1)–(4.3)].

Let us now average the pressure over a period as in Eq. (3.59). We find

$$\langle p_0\rangle=\epsilon_0\left\{\frac{8}{3}\left[\frac{k^2-2}{k^4}\left(1-\frac{E(k)}{K(k)}\right)+\frac{1}{k^2}\right]-1\right\}$$

$$\text{for } 0\leqslant\eta_0\leqslant\sqrt{2},$$

$$\langle p_0\rangle=\epsilon_0\left\{\frac{8}{3}\left[(1-2k^2)\left(1-\frac{E(k)}{K(k)}\right)+k^2\right]-1\right\}\text{ for }\eta_0\geqslant\sqrt{2}. \tag{4.25}$$

The dimensionless energy ϵ_0 tends to 1/4 both as $\eta_0\to 0$ and $\eta_0\to\sqrt{2}$, in both cases we find using Eq. (4.25)

$$\frac{\langle p_0\rangle}{\epsilon_0}\to -1-\frac{16}{3\ln|\frac{1}{4}-\epsilon_0|}+O(\epsilon_0-\tfrac{1}{4}). \tag{4.26}$$

This result is recognized as vacuum behavior in this limit.

For $\eta_0\to 1$, Eq. (4.25) yields

$$\frac{\langle p_0\rangle}{\epsilon_0}\underset{\eta_0\to 1}{\sim} O(\eta_0-1)^2. \tag{4.27}$$

That is a dust-type behavior, which is consistent with the small amplitude limit of the unbroken symmetry case studied before.

Finally, for $\eta_0\to\infty$, when the zero mode is released from high up the potential hill, we find that the pressure approaches radiation behavior (from above)

$$\frac{\langle p_0\rangle}{\epsilon_0}\underset{\eta_0\to\infty}{\sim}\frac{1}{3}+\frac{4}{3}\left[\frac{1}{\sqrt{2}}-1+\left(2-\frac{1}{\sqrt{2}}\right)\frac{E(1/\sqrt{2})}{K(1/\sqrt{2})}\right]\frac{1}{\eta_0^2}+O\left(\frac{1}{\eta_0^4}\right)$$

$$=\frac{1}{3}+\frac{0.86526\ldots}{\eta_0^2}+O\left(\frac{1}{\eta_0^4}\right). \tag{4.28}$$

Figure 3 shows $\langle p_0\rangle/\varepsilon_0$ vs ε_0.

As mentioned before, we expect that for $\eta_0\ll 1$ the conclusion will be modified dramatically by the quantum corrections.

B. Numerical results

In the region $\eta_0\approx 1$ the analytic estimates are a good approximation for large times and weak couplings. We have studied numerically many different cases with $\eta_0\geqslant 0.5$ and weak coupling and confirmed the validity of the analytic estimates. These cases are qualitatively similar to the unbroken symmetry case with almost undamped oscillations for a long time compatible with the weak coupling approximation and when $g\Sigma(\tau)$ grows by parametric amplification to be of order 1 with a consequently large number of produced particles and the evolution of the zero mode damps out.

However, as argued above, for $\eta_0\ll 1$ the analytic approximation will not be very reliable because the quantum fluctuations grow on a time scale of a period or so (depending on the coupling) and the back-reaction term cannot be neglected. Thus, this region needs to be studied numerically.

We numerically solved Eqs. (2.43) and (2.44) with the initial conditions (2.42), (2.45)–(2.47). The numerical routines are the same as in the unbroken symmetry case. Again we tested cutoffs $\Lambda/|M_R|=100,70,50,20$ and for very small couplings (which is the case of interest, $g=10^{-6}\ldots g=10^{-12}$) we found no appreciable cutoff dependence, with results that are numerically indistinguishable even for cutoffs as small as $q_c\approx 2$. The typical numerical error both in the differential equations and the integrals are the same as in the unbroken case, less than one part in 10^9.

We begin the numerical study by considering first the case of very small coupling and $\eta_0\ll 1$; later we will deal with the case of larger couplings and initial values of the zero mode. Figure 4(a) shows $\eta(\tau)$ vs τ for $\eta_0=10^{-5}$, $g=10^{-12}$. In this case we see that within one period of the classical evolution of the zero mode, $g\Sigma(\tau)$ becomes of order 1, the quantum fluctuations become nonperturbatively large and the approximation valid for early times and weak

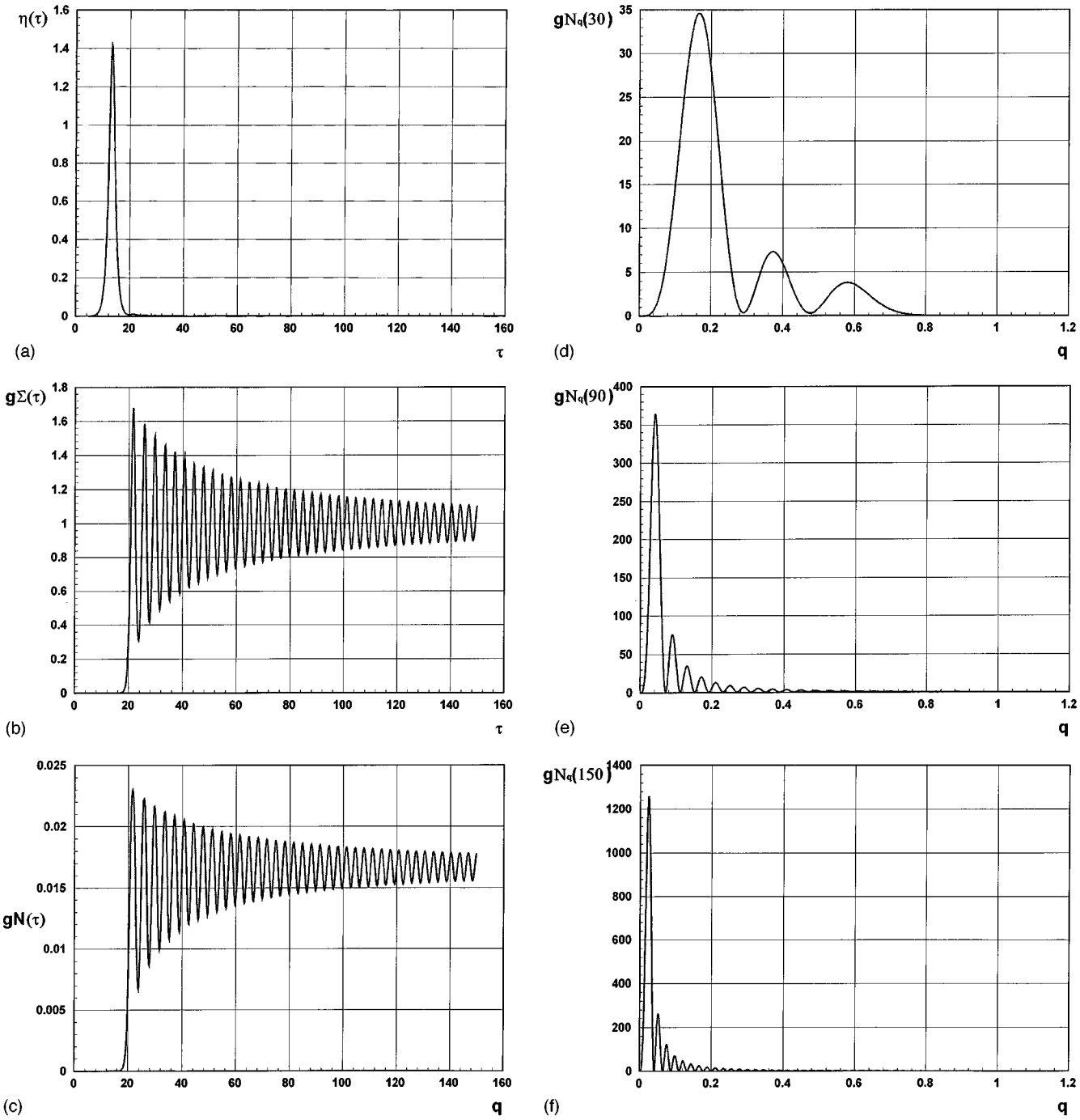

FIG. 4. (a) $\eta(\tau)$ vs τ for the broken symmetry case with $\eta_0 = 10^{-5}$, $g = 10^{-12}$. (b) $g\Sigma(\tau)$ for the same values of the parameters as in (a). (c) $g\mathcal{N}(\tau)$ for the same parameters as in (a). (d) $gN_q(\tau)$ vs q for $\tau = 30$ for the same values of parameters as (a). (e) $gN_q(\tau)$ vs q for $\tau = 90$ for the same values of parameters as (a). (f) $gN_q(\tau)$ vs q for $\tau = 150$ for the same values of parameters as (a). (g) $\mathcal{M}^2(\tau)$ vs τ for the same parameters as (a). (h) $\varepsilon_{cl}(\tau)$ vs τ for the same parameters as (a). (i) $\varepsilon_N(\tau)$ vs τ for the same parameters as (a). (j) $\varepsilon_C(\tau)$ vs τ for the same parameters as (a). (k) $(\lambda_R/2|M_R|^4)p(\tau)$ for the same values of the parameters as in (a). Asymptotically the average over a period gives $p_\infty = \varepsilon/3$.

couplings breaks down. Figure 4(b) shows $g\Sigma(\tau)$ and Fig. 4(c) shows $g\mathcal{N}(\tau)$ vs τ for these parameters. We find that only the wave vectors in the region $0 < q < 1$ are important, i.e., there is only one unstable band whose width remains constant in time. This is seen in Figs. 4(d)–(f), which show the particle number (defined with respect to the initial state) as a function of wave vector for different times, $gN_q(\tau = 30)$, $gN_q(\tau = 90)$, $gN_q(\tau = 150)$, respectively. Although the analytic approximation breaks down, the prediction equation (4.7) for the band width agrees remarkably well with the numerical result. As in the unbroken case, the band develops structure but its width is constant throughout the evolution. As can be seen in these figures the peak of the distribution becomes higher, narrower, and moves towards smaller values of q. The concentration of particles at very low momentum is a consequence of the excitations being

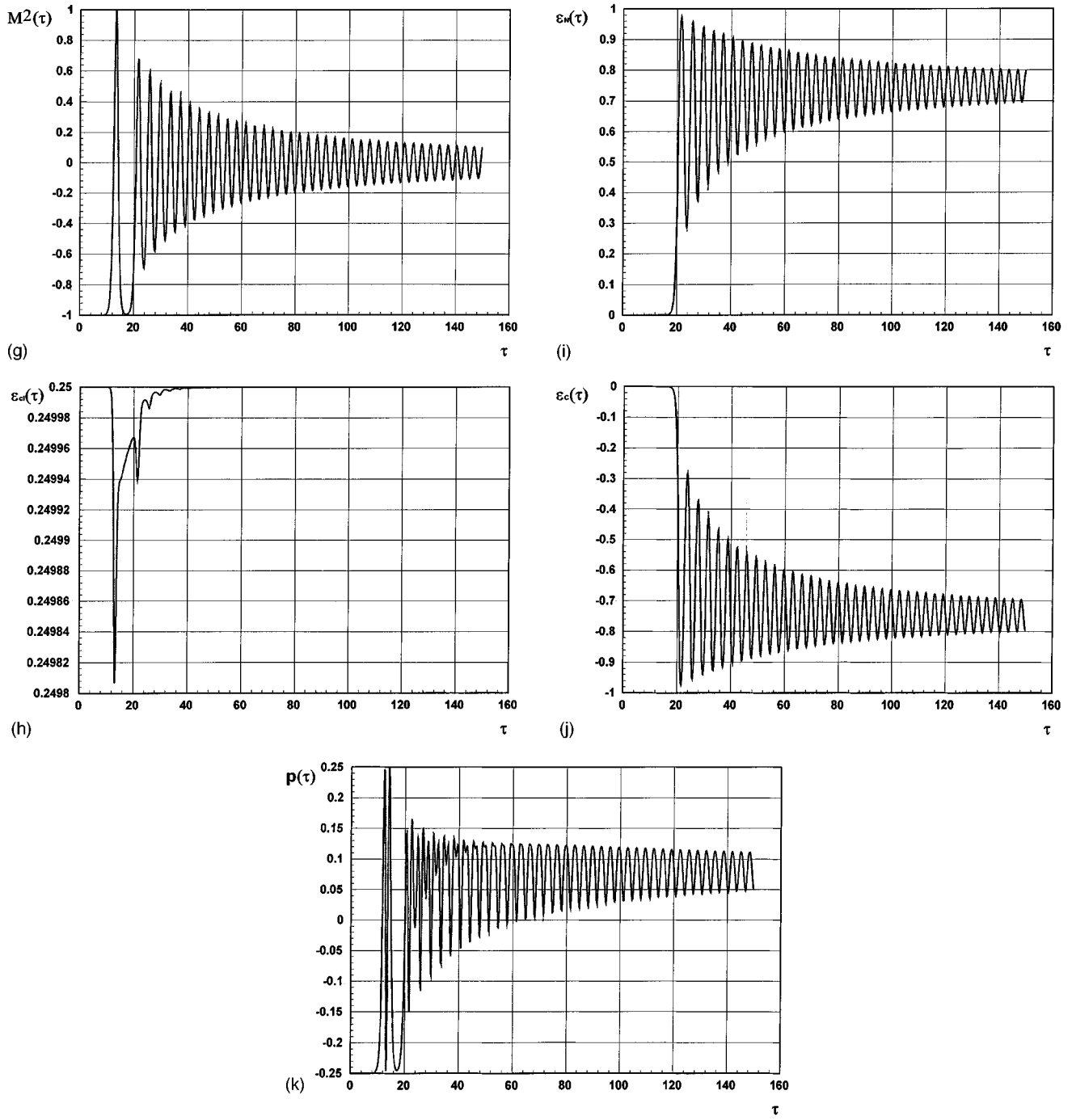

FIG. 4 (*Continued*).

effectively massless in the broken symmetry case. The features are very distinct from the unbroken symmetry case, in which the peak approaches $q \approx 0.5$.

We found in all cases that the asymptotic behavior corresponds to

$$\mathcal{M}^2(\tau) = -1 + \eta^2(\tau) + g\Sigma(\tau) \overset{\lim \tau \to \infty}{\rightarrow} 0. \qquad (4.29)$$

This is a consistent asymptotic solution that describes massless ''pions'' and broken symmetry in the case $\eta(\infty) \neq 0$.

For times $\tau \approx 100-150$ the value of the zero mode is somewhat larger than the initial value: $\eta(\tau = 150) \approx 2 \times 10^{-5}$. This result, when combined with the result that the average of the effective mass approaches zero, is clearly an indication that the symmetry is *broken*. We found numerically that the final value of the zero mode depends on the initial value and the coupling and we will provide numerical evidence for this behavior below.

Figure 4(a) presents a puzzle. Since the zero mode begins very close to the origin with zero derivative and *ends up* very close to the origin with zero derivative, the classical energy of the zero mode is conserved. At the same time, however, the dynamical evolution results in copious particle production as can be seen from Fig. 4(c). We have shown in Sec. II E that the total energy is conserved and this was numeri-

cally checked within the numerical error. Thus the puzzle: how is it possible to conserve the *total* energy, conserve the classical zero mode energy, and at the same time create $O(1/g)$ particles? The answer is that there is a new term in the total energy that acts as a ''zero point energy'' that diminishes during the evolution and thus maintains total energy conservation with particle production. The most important contribution to the energy arises from the zero mode and the unstable modes $0<q<q_u$. The energy and pressure are given by (adjusting the constant $\mathcal{C}$ such that the energy coincides with the classical value)

$$\varepsilon=\frac{2|M_R|^4}{\lambda_R}\{\varepsilon_{cl}+\varepsilon_N+\varepsilon_C+O(g)\}, \tag{4.30}$$

$$\varepsilon_{cl}=\frac{\dot{\eta}^2}{2}+\frac{1}{4}(\eta^2-1)^2, \tag{4.31}$$

$$\varepsilon_N=2g\int_0^{q_u}q^2dq\Omega_q N_q(\tau), \tag{4.32}$$

$$\varepsilon_C=\frac{g}{2}\Sigma(\tau)\left[-1-\eta_0^2+\mathcal{M}^2(\tau)-\frac{g}{2}\Sigma(\tau)\right], \tag{4.33}$$

$$p=\frac{2|M_R|^4}{\lambda_R}\left\{g\int_0^{q_u}q^2dq\left[\frac{q^2}{3}|\varphi_q(\tau)|^2+|\dot{\varphi}(\tau)|^2\right]+\dot{\eta}^2+O(g)\right\}-\varepsilon, \tag{4.34}$$

$$\mathcal{M}^2(\tau)=-1+\eta^2(\tau)+g\Sigma(\tau), \tag{4.35}$$

where $\mathcal{M}(\tau)^2$ is the effective squared mass of the $N-1$ ''pions'' and again $O(g)$ stands for perturbatively small terms of order g. The terms displayed in Eq. (4.31)–(4.34) are all of $O(1)$ during the preheating stage.

We find that whereas ε_N grows with time, the term ε_C becomes negative and decreases. In all the cases that we studied, the effective mass $\mathcal{M}(\tau)$ approaches zero asymptotically; this is seen in Fig. 4(g) for the same values of the parameters as in Figs. 4(a)–(c). This behavior and an asymptotic value $\eta_\infty\neq 0$ are consistent with broken symmetry and massless pions by Goldstone's theorem. The term ε_C in Eq. (4.33) can be identified with the ''zero'' of energy. It contributes to the equation of state as a vacuum contribution, that is, $p_C=-\varepsilon_C$ and becomes negative in the broken symmetry state. It is this term that compensates for the contribution to the energy from particle production.

This situation is generic for the cases of interest for which $\eta_0\ll 1$; such is the case for the slow roll scenario in inflationary cosmology. Figures 4(h)–4(k) show $\varepsilon_{cl}(\tau)$ vs τ, $\varepsilon_N(\tau)$ vs τ, $\varepsilon_C(\tau)$ vs τ, and $(\lambda_R/2|M_R|^4)p(\tau)$ vs τ for the same values of parameters as Fig. 4(a). The pressure has a remarkable behavior. It begins with $p=-\varepsilon$ corresponding to vacuum domination and ends asymptotically with a radiationlike equation of state $p=\varepsilon/3$. A simple explanation for radiationlike behavior would be that the equation of state is dominated by the quantum fluctuations which as argued above correspond to massless pions and, therefore, ultrarelativistic. It must be noted that we obtain a radiationlike equation of state in spite of the fact that the the distribution is out of equilibrium and far from thermal as can be seen from Figs. 4(d)–4(f).

An important question to address at this point is: why does the zero mode reach an asymptotic value *different* from the minimum of the effective potential? The answer to this question is that the effective potential is an irrelevant quantity to study the dynamics [3,11]. Once there is profuse particle production, a feature completely missed by the effective potential, the zero mode evolves in a nonequilibrium bath of these excitations. Through the time evolution, more of these particles are produced and the zero mode evolves in a highly excited, nonequilibrium state. Furthermore we have seen in detail that this mechanism of particle production modifies dramatically the zero point origin of energy and therefore the minimum of the effective action, which is now the appropriate concept to use. The final value reached by the zero mode in the evolution will be determined by all of these *nonperturbative* processes, and only a full numerical study will capture the relevant aspects. As we have argued above, approximations based on Mathieu-type equations or the WKB approximation are bound to miss important details and will lead to a completely different evolution.

V. SYMMETRY RESTORATION AT PREHEATING?

The numerical result depicted by Figs. 4(a)–4(c), which are very similar to results obtained previously [3], has motivated the suggestion that the growth of quantum fluctuations is so strong that the nonequilibrium fluctuations restore the symmetry [1,13]. The argument is that the nonequilibrium fluctuations given by the term $\lambda\langle\psi^2(t)\rangle$ in Eq. (2.20) for the mode functions grow exponentially and eventually this term overcomes the term $-|m^2|$ leading to an effective potential with a *positive* mass squared for the zero mode [see Eq. (2.19)].

Although this is a very interesting suggestion, it is *not* borne out by our numerical investigation. The signal for broken or restored symmetry is the final value of the zero mode when the system reaches an equilibrium situation. Any argument about symmetry restoration based solely on the dynamics of the fluctuation term $\lambda\langle\psi^2(t)\rangle$ is incomplete if it does not address the dynamics of the zero mode. In particular, for the case of Figs. 4(a)–(c), the initial value of the zero mode $\eta_0\neq 0$ and the final value is very close to the initial value but still *different from zero*.

At the same time, the asymptotic effective mass of the ''pions'' is on average zero. Clearly, this is a signal for symmetry breaking. Because the initial and final values of the order parameter are so small on the scale depicted in the figures, one is tempted to conclude that the symmetry originally broken by a very small value of the order parameter is restored asymptotically by the growth of nonequilibrium fluctuations. To settle this issue we show a different set of parameters in Figs. 5(a) and 5(b) that unambiguously show that the final value of the order parameter $\eta_\infty\neq 0$, while the effective mass of the pions $\mathcal{M}(\tau)\to 0$. Here, $\eta_0=0.01$ and $g=10^{-5}$, and asymptotically we find $\eta(\tau=150)\approx 0.06$, the average of the effective mass squared $\mathcal{M}^2(\tau)=0$, and the symmetry is broken, despite the fact that the fluctuations

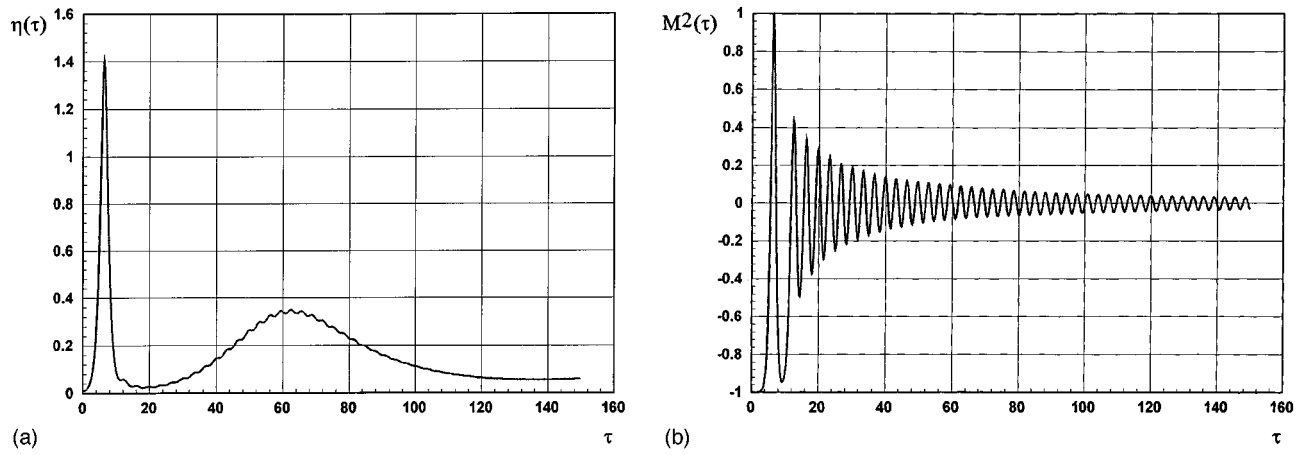

FIG. 5. (a) $\eta(\tau)$ vs τ for the broken symmetry case with $\eta_0=10^{-2}$, $g=10^{-5}$. (b) $\mathcal{M}^2(\tau)$ vs τ for the same parameters as (a).

have grown exponentially and a number of particles $O(1/g)$ has been produced.

The reason that the symmetry is *not* restored is that when the effective mass becomes positive, the instabilities shut off and the quantum fluctuations become small. When this happens $g\Sigma$ is no longer of order 1 and the instabilities appear again, producing the oscillatory behavior that is seen in the figures for $g\Sigma(\tau)$ at long times, such that the contributions of the oscillatory terms average to zero. It is rather straightforward to see that there is a self-consistent solution of the equations of motion for the zero mode and the fluctuations with constant η_∞ and $\mathcal{M}^2(\infty)=0$. Equation (2.43) takes the asymptotic form [3]

$$\eta_\infty[-1+\eta_\infty^2+g\Sigma(\infty)]=0.$$

In addition, Eq. (2.44) yields when $\mathcal{M}(\infty)^2=0$,

$$\varphi_q(\tau) \underset{\tau\to\infty}{\sim} A_q e^{-iq\tau}+B_q e^{iq\tau},$$

where A_q and B_q depend on the initial conditions and g. We get from Eqs. (2.42) and (2.53),

$$\eta_\infty^2=1-4g\int_0^\infty \frac{q^2\Omega_q}{q^2+\Omega_q^2}N_q(\infty)dq-gS(\eta_0), \qquad (5.1)$$

where

$$S(\eta_0)\equiv\frac{1}{4}(1-\eta_0^2)\left[\ln\frac{1-\eta_0^2}{4}-\frac{\pi}{2}\right]+\frac{1}{2}(1+\eta_0^2)\times\left[\mathrm{ArgTh}\sqrt{\frac{1-\eta_0^2}{2}}-\arctan\sqrt{\frac{1-\eta_0^2}{2}}\right].$$

We see that the value of η_∞ depends on the initial conditions. Whereas the last term in Eq. (5.1) is perturbatively small, the contribution from the produced particles is nonperturbatively large, as $N_q(\infty)\approx 1/g$ for the unstable wave vectors. Thus, the asymptotic value of the zero mode is drastically modified from the tree level vacuum expectation value (VEV) (in terms of renormalized parameters) because of the profuse particle production because of the nonequilibrium growth of fluctuations.

Another way to argue that the symmetry is indeed broken in the final state is to realize that the distribution of ''pions'' at late times will be different than the distribution of the quanta generated by the fluctuations in the σ field, if for no other reason than that the pions are asymptotically massless while the σ quanta are massive, as long as η_∞ is different from zero. If the symmetry were restored during preheating, these distributions would have to be identical.

The conclusion is that the final value of the zero mode depends strongly on the initial conditions and couplings, though symmetry restoration can take place for other situations.

A consistent study of the evolution of the zero mode and quantum fluctuations determines what happens in each case [29]. Thus we emphasize that the ultimate test for symmetry restoration is asymptotic in time evolution of the zero mode, which is the order parameter for symmetry breaking.

VI. THE REHEATING TEMPERATURE

The arena in which these results become important is that of inflationary cosmology. In particular, the process of preheating is of vital importance in understanding how the bigbang cosmology is regained at the end of inflation, i.e., the reheating mechanism.

While our analysis has been entirely a Minkowski space one, we can make some comments concerning the reheating temperature. However, a more detailed analysis incorporating the expanding universe must eventually be done along the lines suggested in this work, to get more accurate results.

Since the particles created during the preheating stage are far from equilibrium, thermalization and equilibration will be achieved via collisional relaxation. In the approximation that we are studying, however, collisions are absent and the corresponding contributions are of $O(1/N)$ [9]. The difficulty with the next order calculation and incorporation of scattering terms is that these are nonlocal in time and very difficult to implement numerically.

However, we can obtain an estimate for the reheating temperature under some reasonable assumptions: in the cosmological scenario, *if* the equilibration time is shorter than the inverse of the expansion rate H, then there will not be appreciable redshifting of the temperature because of the ex-

pansion and we can use our Minkowski space results.

The second assumption is that the time scales between particle production and thermalization and equilibration are well separated. Within the large N approximation this is clearly correct because at large N, scattering processes are suppressed by $1/N$. If these two time scales are widely separated then we can provide a fairly reliable estimate of the reheating temperature as follows.

Equilibration occurs via the *redistribution* of energy and momentum via elastic collisional processes. Assuming that thermalization occurs on time scales larger than that of particle production and parametric amplification, then we can assume energy conservation in the scattering processes. Although a reliable and quantitative estimate of the reheating temperature can only be obtained after a detailed study of the collisional processes which depend on the interactions, we can provide estimates in two important cases. If the scattering processes do not change chemical equilibrium, that is, conserve particle number, the energy per particle is conserved. Since the energy (density) stored in the nonequilibrium bath and the total number of particles per unit volume are, as shown in the previous sections:

$$\varepsilon \approx \frac{|M_R|^4}{\lambda_R}, \tag{6.1}$$

$$N \approx \frac{|M_R|^3}{\lambda_R}, \tag{6.2}$$

with proportionality constants of order 1, we can estimate the reheating temperature to be

$$\frac{\varepsilon}{N} \approx T \approx |M_R|. \tag{6.3}$$

Here $|M_R|$ is the inflaton mass. This is consistent with previous results [3].

This result seems puzzling, since naively one would expect $\varepsilon \approx T_R^4; N \approx T_R^3$ but the powers of λ do not match. This puzzle arises from intuition based on an ultrarelativistic-free particle gas. However, the ''medium'' is highly excited with a large density of particles and the ''in medium'' properties of the equilibrated particles may drastically modify this result as is known to happen in most theories at high temperature, where the medium effects are strong and perturbation theory breaks down requiring hard thermal loop resummation.

In the case in which the collisional processes do not conserve particle number and, therefore, change chemical equilibrium, the only conserved quantity is the energy. Such is the case for massless particles interacting with a quartic couplings for example, or higher order processes in a quartic theory with massive particles. Processes in which $3 \to 1$ conserving energy and momentum can occur. The inverse process $1 \to 3$ occurs with far less probability since the high momentum modes are much less populated than the low momentum modes in the unstable bands. In this case only energy is conserved whereas the total number of particles is *not conserved* and in this case an estimate of the reheating temperature compares the energy density in the bath of produced particles to that of an ultrarelativistic gas in equilibrium at temperature T_R,

$$\varepsilon \approx \frac{|M_R|^4}{\lambda_R} \approx T_R^4, \tag{6.4}$$

leading to the estimate

$$T_R \approx \frac{|M_R|}{\lambda_R^{1/4}}. \tag{6.5}$$

Thus we can at least provide a bound for the reheating temperature

$$|M_R| \leqslant T_R \leqslant \frac{|M_R|}{\lambda} \tag{6.6}$$

and a more quantitative estimate requires a deeper understanding of the collisional processes involved.

Within the large N approximation, scattering terms will appear at order $1/N$ and beyond. The leading contribution $O(1/N)$ to collisional relaxation conserves particle number in the unbroken symmetry state because the product particles are massive. This can be seen from the fact that the self-energy to this order is given by the same chain of bubbles that gives the scattering amplitude but with two external legs contracted. All cut diagrams (that give the imaginary part) correspond to $2 \to 2$ processes that conserve particle number because of kinematic reasons. Certainly, at higher order in $1/N$ there will be processes that change chemical equilibrium, but for large N these are suppressed formally. This argument based on the leading collisional contribution in the $1/N$ expansion allows us to provide a further consistent estimate in the unbroken symmetry case (when the produced particles are massive). In this approximation and consistently with energy and particle number conservation we can assume that the final equilibrium temperature is of the order of the typical particle energy before thermalization. Recalling that the unstable band remains stable during the evolution with the peak shifting slightly in position we can estimate the typical energy per particle by the position of the peak in the distribution at q_1, and use the analytical estimate for the peak given in Sec. II. Restoring the units we then obtain the estimate

$$T_R \approx |M_R| q_1 \approx |M_R| \frac{\eta_0}{2} \approx \sqrt{\frac{\lambda_R}{8}} \Phi_0, \tag{6.7}$$

which displays the dependence on η_0 explicitly. Equation (6.7) is an improvement of the simple estimate (6.3).

It must be noticed that the peak in the momentum distribution decreases with time for $t > t_{\rm reh}$ [see Figs. 2(f)–2(h)]. This drift follows from the nonlinear interaction between the modes. For the case of Fig. 2, one sees that T_R reduces by approximately a factor 3 with respect to the value (6.7).

The large N model studied in this article is not a typical model used in inflationary cosmology, and since we want to make a quantitative statement for inflationary scenarios

(within the approximation of only considering Minkowski space) we now study a model that incorporates other scalar fields coupled to the inflaton.

The simplest model [4,5] contains, in addition to the inflaton, a lighter scalar field σ with a $g\sigma\Phi^2$ coupling. That is, we consider the Lagrangian [3],

$$\mathcal{L}=-\frac{1}{2}\Phi(\partial^2+m^2+g\sigma)\Phi-\frac{\lambda}{4!}\Phi^4 -\frac{1}{2}\sigma(\partial^2+m_\sigma^2)\sigma-\frac{\lambda_\sigma}{4!}\sigma^4. \tag{6.8}$$

We will consider again the preheating regime of weak couplings and early times such that we can neglect the back reaction of the quantum fluctuations of the σ field as well as the back reaction of the quantum fluctuations of the inflation itself, focusing only on the parametric growth of the σ fluctuations in the unbroken symmetry case. The mode equations for the σ field take the form

$$\left[\frac{d^2}{dt^2}+k^2+m_\sigma^2+g\phi^2(t)\right]V_k(t)=0\,. \tag{6.9}$$

In dimensionless variables this equation becomes

$$\left[\frac{d^2}{d\tau^2}+q^2+\left(\frac{m_\sigma}{m}\right)^2+\frac{6g}{\lambda}\eta^2(\tau)\right]V_k(\tau)=0\,. \tag{6.10}$$

In the short time approximation we can replace $\eta(\tau)$ by the classical form (3.1). We then find a Lamé equation which admits closed form solutions for [18]

$$\frac{12g}{\lambda}=n(n+1),\quad n=1,2,3,\ldots. \tag{6.11}$$

Although these are not generic values of the couplings, the solubility of the model and the possibility of analytic solution for these cases make this study worthwhile. In the simplest case, ($n=1,6\ g=\lambda$), there is only one forbidden band for $q^2>0$. It goes from $q^2=1-(m_\sigma/m)^2$ to $q^2=1-(m_\sigma/m)^2+\eta_0^2/2$. That is,

$$\text{forbidden band:}\quad m^2-m_\sigma^2<k^2<m^2-m_\sigma^2+\frac{\lambda}{4}\Phi_0^2\,. \tag{6.12}$$

The Floquet index in this forbidden band takes the form

$$F(q)=2iK(k)Z(2K(k)v)\pm\pi, \tag{6.13}$$

where now v and q are related by the equation

$$q^2=1-\left(\frac{m_\sigma}{m}\right)^2+\frac{\eta_0^2}{2}\mathrm{cn}^2(2K(k)v,k), \tag{6.14}$$

and $0\leqslant v\leqslant 1/2$.

The imaginary part of the Floquet index is now maximal at $q_1^2=1-(m_\sigma/m)^2+\eta_0^2/4$ and we can use this value to provide an estimate for the reheating temperature in this model in the same manner as for Eq. (6.7), yielding the following estimate for the reheating temperature

$$T_{\mathrm{reh}}\simeq\sqrt{m^2-m_\sigma^2+\frac{\lambda}{8}\Phi_0^2}. \tag{6.15}$$

In the special case $m_\sigma=m=|M_R|$, we recover Eq. (6.7), as expected.

Again, the nonlineal field evolution for $t>t_{\mathrm{reh}}$ decreases T_{reh}. In the third reference under [3], we found for late times a T_{reh} ten times smaller than the value (6.15) for $g=1.6\pi^2$.

The estimates on the reheating temperature provided above should not be taken rigorously, but as an approximate guide. A consistent estimate of the reheating temperature and the thermalization time scales would, in principle, involve setting up a Boltzmann equation [5]. Under the assumption of a separation between the preheating and thermalization time scales one could try to use the distribution functions N_q at the end of the preheating stage as input in the kinetic Boltzmann equation. However, we now argue that such a kinetic description is *not valid* to study thermalization. A kinetic approach based on the Boltzmann equation, with binary collisions, for example, would begin by writing the rate equation for the distribution of particles

$$\dot{N}_k\propto\lambda^2\int d^3k_1d^3k_2d^3k_3\delta^4(k_1+k_2+k_3+k) \times[(1+n_k)(1+n_{k_1})n_{k_2}n_{k_3}n_kn_{k_1}(1+n_{k_2})(1+n_{k_3})]. \tag{6.16}$$

However, this equation is only valid in the *low density* regime. In particular for the case under study, the occupation numbers for wave vectors in the unstable bands are nonperturbatively large $\propto 1/\lambda$ and one would be erroneously led to conclude that thermalization occurs on the same time scale or *faster than* preheating.

Clearly such a statement would be too premature. Without a separation of time scales, the kinetic approach is unwarranted. The solution of the Boltzmann equation provides a partial resummation of the perturbative series which is valid whenever the time scales for relaxation are much longer than the microscopic time scales [27], in this case that of particle production.

In the case under study there is an expansion parameter $1/N$ and clearly these scattering terms are subleading in this formal limit, so that the separation of time scales is controlled. In the absence of such an expansion parameter, some resummation scheme must be invoked to correctly incorporate scattering. In particular when the symmetry is broken, the asymptotic excitations are Goldstone bosons, the medium is highly excited but with very long-wavelength Goldstones and these have very small scattering cross sections. Such a resummation is also necessary in the large temperature limit of field theories in equilibrium. In this case the perturbative expansion of the scattering cross section involves powers of $\lambda T/m$ with m being the mass. A correct resummation of the (infrared) divergent terms leads to $\lambda(T)\to m/T$ in the large T/m limit [28]. In particular the $1/N$ corrections in the formal large N limit involve such a resummation, but in the nonequilibrium situation, the numerical implementation of this resummation remains a formidable problem.

VII. CONCLUSIONS

It is clear that preheating is both an extremely important process in a variety of settings, as well as one involving very delicate analysis. In particular, its nonperturbative nature renders any treatment that does not take into account effects such as the quantum back reaction due to the produced particles, consistent conservation (or covariant conservation) of the relevant quantities and Ward identities, incapable of correctly describing the important physical phenomena during the preheating stage.

In this work, we dealt with these issues by using the O(N) vector model in the large N limit. This allows for a controlled nonperturbative approximation scheme that conserves energy and the proper Ward identities, to study the nonequilibrium dynamics of scalar fields. Using this model we were able to perform a full analysis of the evolution of the zero mode as well as of the particle production during this evolution.

Our results are rather striking. We were able to provide analytic results for the field evolution as well as the particle production and the equation of state for all these components in the weak coupling regime and for times for which the quantum fluctuations, which account for back-reaction effects, are small. What we found is that, in the unbroken symmetry situation, the field modes satisfy a Lamé equation that corresponds to a Schrödinger equation with a two-zone potential. There are two allowed and two forbidden bands, which is *decidedly* unlike the Mathieu equation used in previous analysis [1,12]. The difference between an equation with two forbidden bands and one with an infinite number is profound. We were also able to estimate analytically the time scale at which preheating would occur by asking when the quantum fluctuations as calculated in the absence of back reaction would become comparable to the tree level terms in the equations of motion. The equations of state of both the zero mode and ''pions'' were calculated and were found to be describable as polytropes. These results were then confirmed by numerical integration of the equations, and we found that the analytic results were in great agreement with the numerical ones in their common domain of validity.

When the O(N) symmetry is spontaneously broken, more subtle effects can arise, again in the weak coupling regime. If the zero mode starts off very near the origin, then the quantum back reaction grows to be comparable to the tree level terms within one or at most a few oscillations even for very weak coupling. In this case the periodic approximation for the dynamics of the zero mode breaks down very early on and the full dynamics must be studied numerically.

When numerical tools are brought to bear on this case we find some extremely interesting behavior. In particular, there are situations in which the zero mode starts near the origin (the initial value depends on the coupling) and then in one oscillation, comes back to almost the same location. However, during the evolution it has produced $1/g$ particles. Given that the total energy is conserved, the puzzle is to find where the energy came from to produce the particles. We found the answer in a term in the energy density that has the interpretation of a ''vacuum energy'' that becomes *negative* during the evolution of the zero mode and whose contribution to the equation of state is that of ''vacuum.'' The energy given up by this term is the energy used to produce the particles.

This example also allows us to study the possibility of symmetry restoration during preheating [1,13,26]. While there have been arguments to the effect that the produced particles will contribute to the quantum fluctuations in such a way as to make the effective mass squared of the modes positive and thus restore the symmetry, we argued that they were unfounded. Whereas the effective squared mass oscillates, taking positive values during the early stages of the evolution, its asymptotic value is zero, compatible with Goldstone bosons as the asymptotic states.

Furthermore, this says nothing about whether the symmetry is restored or not. This is signaled by the final value of the zero mode. In all the situations examined here, the zero mode is driven to a *nonzero* final value. At this late time, the ''pions'' become massless, i.e., they truly are the Goldstone modes required by Goldstone's theorem.

The arguments presented in favor of symmetry restoration rely heavily on the effective potential. We have made the point of showing explicitly why such a concept is completely irrelevant for the nonequilibrium dynamics when profuse particle production occurs and the evolution occurs in a highly excited, out of equilibrium state.

Finally, we dealt with the issue of how to use our results to calculate the reheating temperature due to preheating in an inflationary universe scenario. Since our results are particular to Minkowski space, we need to assume that preheating and thermalization occur on time scales shorter than the expansion time, i.e., H^{-1}. We also need to assume that there is a separation of time scale between preheating and thermalization. Under these assumptions we can estimate the reheating temperature as $T_{\rm reh} \propto |M_R|$ in the case when the collisional processes maintain chemical equilibrium (conserve particle number) or $T_{\rm reh} \propto |M_R|/\lambda^{1/4}$ in the case in which particle number is not conserved in the collisions (such is the case for massless particles in general).

We have made the important observation that due to the large number of long-wavelength particles in the forbidden bands, a kinetic or Boltzmann equation approach to thermalization is *inconsistent* here. A resummation akin to that of hard thermal loops, that consistently arises in the next order in $1/N$ must be employed. In equilibrium such a resummation shows that the scattering cross section for soft modes is perturbatively small despite their large occupation numbers.

There is a great deal left to explore. Clearly the first step from this work would be to generalize what we have done to include the expansion of the Universe. This should be done both in order to understand preheating in more detail, as well as to understand the evolution of the scalar field during the inflationary period. Further steps should certainly include trying to incorporate thermalization effects systematically within the $1/N$ expansion.

As we were finishing the writeup of this work, we learned about complementary work by Cooper, Kluger, Habib, and Mottola [30] who studied similar issues in the broken symmetry phase with results that are consistent with those found by us.

ACKNOWLEDGMENTS

D.B. thanks the N.S.F. for support through Grant Nos. PHY-9302534 and INT-9216755. R.H. was supported by

DOE Grant No. DE-FG02-91-ER40682. D.B. and R.H. would also like to acknowledge LPTHE at the Université de Paris VI for its hospitality during part of this work. D.B. and H.J.d.V. would like to thank S. Habib and E. Mottola for stimulating conversations and for sharing with them results of their work prior to distribution. D.B. thanks the Pittsburgh Supercomputer Center for Grant No. PHY950011P. LPTHE is Laboratoire Associé au CNRS UA280.

APPENDIX: SOME RESULTS ON ELLIPTIC FUNCTIONS

Here we detail some of the derivations used in the main text for the analytic results.

1. The unbroken symmetry case

We derive here the solutions of the mode equation (3.3),

$$\left[\frac{d^2}{d\tau^2}+q^2+1+\eta_0^2-\eta_0^2\,\mathrm{sn}^2(\tau\sqrt{1+\eta_0^2},k)\right]\varphi_q(\tau)=0, \tag{A1}$$

where $k=\eta_0/\sqrt{2(1+\eta_0^2)}$.

It is convenient to express the Jacobi sine in terms of the Weierstrass $\mathcal{P}$ function through [25]

$$\mathrm{sn}^2(\tau\sqrt{1+\eta_0^2},k)=\frac{1}{k^2\mathrm{sn}^2[\tau\sqrt{1+\eta_0^2}+iK'(k),k]}$$
$$=\frac{1}{k^2(e_1-e_3)}\left[\mathcal{P}\left(\frac{\tau\sqrt{1+\eta_0^2}+iK'(k)}{\sqrt{e_1-e_3}}\right)-e_3\right], \tag{A2}$$

$$k^2=\frac{e_2-e_3}{e_1-e_3}. \tag{A3}$$

We assume that the discriminant Δ of the function $\mathcal{P}$ is here positive and that the roots e_1,e_2,e_3 of the cubic equation obeying $e_1+e_2+e_3=0$ are ordered as

$$e_3<e_2<0<e_1. \tag{A4}$$

In addition, without any loss of generality we choose $e_1-e_3=1+\eta_0^2$. With such a choice we find the roots to be: $3e_1=\frac{3}{2}\eta_0^2+2, 3e_2=-1$, and $3e_3=-\frac{3}{2}\eta_0^2-1$.

Collecting all factors the mode equation (A1) becomes

$$\left[\frac{d^2}{d\tau^2}+q^2+\tfrac{1}{3}-2\,\mathcal{P}(\tau+\omega')\right]\varphi_q(\tau)=0, \tag{A5}$$

where $\omega'\equiv iK'(k)/\sqrt{1+\eta_0^2}$.

Equation (A5) is a Lamé equation that can be solved in closed form in terms of Weierstrass functions. The solution is [23]

$$U_q(\tau)=\frac{\sigma(\tau+\omega'+z)\sigma(\omega')}{\sigma(\tau+\omega')\sigma(\omega'+z)}e^{-\tau\zeta(z)}, \tag{A6}$$

where z is defined through

$$\mathcal{P}(z)=-\tfrac{1}{3}-q^2, \tag{A7}$$

$\sigma(x)$ and $\zeta(x)$ are Weierstrass functions. We normalize the functions $U_q(\tau)$ according to Eq. (3.5).

Changing τ by $-\tau$ in Eq. (A6) provides an independent solution of Eq. (A5).

Equation (A7) maps the real q^2 axis into the sides of the fundamental square in the z plane [26,30]. That is,

$$z=\beta,\quad 0\leqslant\beta\leqslant\omega,\quad -\infty\leqslant q^2\leqslant-1-\frac{\eta_0^2}{2},$$

$$z=\omega+i\alpha,\quad 0\leqslant\alpha\leqslant\omega'/i,\quad -1-\frac{\eta_0^2}{2}\leqslant q^2\leqslant 0,$$

$$z=\omega'+\beta,\quad \omega\geqslant\beta\geqslant 0,\quad 0\leqslant q^2\leqslant\frac{\eta_0^2}{2},$$

$$z=i\alpha,\quad \omega'/i\geqslant\alpha\geqslant 0,\quad \frac{\eta_0^2}{2}\leqslant q^2\leqslant+\infty, \tag{A8}$$

where $\omega=K(k)/\sqrt{1+\eta_0^2}$. Notice that 2ω is the period in τ of the potential in Eqs. (3.3) and (A5).

The mapping of the real q^2 axis into the sides of the fundamental square in the z plane is made explicit by writing the Weierstrass $\mathcal{P}(z)$ function in terms of Jacobi sn and cn functions [25,30,26]:

$$q^2=-\tfrac{1}{3}-\mathcal{P}(\beta)=\frac{\eta_0^2}{2}-\frac{\eta_0^2+1}{\mathrm{sn}^2(\beta\sqrt{1+\eta_0^2},k)},$$

$$q^2=-\tfrac{1}{3}-\mathcal{P}(\omega+i\alpha)$$
$$=-1-\frac{\eta_0^2}{2}+\left(1+\frac{\eta_0^2}{2}\right)\mathrm{sn}^2(\alpha\sqrt{1+\eta_0^2},k'),$$

$$q^2=-\tfrac{1}{3}-\mathcal{P}(\omega'+\beta)=\frac{\eta_0^2}{2}\,\mathrm{cn}^2(\beta\sqrt{1+\eta_0^2},k),$$

$$q^2=-\tfrac{1}{3}-\mathcal{P}(i\alpha)=-1-\frac{\eta_0^2}{2}+\frac{\eta_0^2+1}{\mathrm{sn}^2(\alpha\sqrt{1+\eta_0^2},k')}. \tag{A9}$$

Here, α and β are real variables. [Recall that $0\leqslant\mathrm{sn}(u,k)\leqslant 1$ for $0\leqslant u\leqslant K(k)$ and that $\mathrm{sn}(u,k)^2+\mathrm{cn}(u,k)^2=1$.]

Generically, a periodic potential possesses an *infinite* number of allowed and forbidden (Floquet) bands that alternate for $0\leqslant q^2<+\infty$. A detailed study of the Floquet indices reveals that this is not the case for Eq. (A1).

Let us now compute the Floquet indices for the mode function (A6). The quasi-periodicity property of the Weierstrass σ functions states that [25,30,26]

$$\sigma(x+2\omega)=-\sigma(x)e^{2(x+\omega)\eta}, \tag{A10}$$

where $\eta\equiv\zeta(\omega)$. Using Eqs. (A10) and (3.4), we find, from Eq. (A6),

$$U_q(\tau+2\omega)=U_q(\tau)\exp\{2[z\eta-\omega\zeta(z)]\},$$

$$F(q)=2i[\omega\zeta(z)-z\eta]. \tag{A11}$$

The quantity q belongs to an allowed band when $2[z\eta-\omega\zeta(z)]$ is purely imaginary and q belongs to a forbidden band when this quantity has a nonzero real part.

Using the properties of the Weierstrass functions [20], we find *two* allowed bands

$$z=i\alpha \text{ and } z=i\alpha+\omega, \tag{A12}$$

with real $\alpha, 0<\alpha<\omega'/i$, and *two* forbidden bands

$$z=\beta \text{ and } z=\beta+\omega', \tag{A13}$$

with real $\beta, 0<\beta<\omega$.

In terms of q^2 the allowed bands correspond to

$$-1-\frac{\eta_0^2}{2}\leqslant q^2\leqslant 0 \text{ and } \frac{\eta_0^2}{2}\leqslant q^2\leqslant +\infty, \tag{A14}$$

and the forbidden bands to

$$-\infty\leqslant q^2\leqslant -1-\frac{\eta_0^2}{2} \text{ and } 0\leqslant q^2\leqslant \frac{\eta_0^2}{2}. \tag{A15}$$

The last forbidden band is for *positive* q^2 and hence *does* contribute to the fluctuation function $\Sigma(\tau)$. $\Sigma(\tau)$ will grow exponentially in time due to the presence of such unstable modes.

Let us investigate the Floquet indices for the forbidden band $0\leqslant q^2\leqslant \eta_0^2/2$. Setting $z=\beta+\omega'$ we find

$$2[z\eta-\omega\zeta(z)]=-\frac{\vartheta_1'\left(\frac{z}{2\omega}\right)}{\vartheta_1\left(\frac{z}{2\omega}\right)}=i\pi-\frac{\vartheta_4'\left(\frac{\beta}{2\omega}\right)}{\vartheta_4\left(\frac{\beta}{2\omega}\right)}, \tag{A16}$$

where we used the relation between the Weierstrass ζ function and the Jacobi ϑ functions [24]

$$\zeta(z)=\frac{\eta}{\omega}z+\frac{1}{2\omega}\frac{\vartheta_1'\left(\frac{z}{2\omega}\right)}{\vartheta_1\left(\frac{z}{2\omega}\right)}. \tag{A17}$$

Here, $\eta\equiv\zeta(\omega)$.

In summary, we have on the forbidden band $0\leqslant q^2\leqslant \eta_0^2/2$,

$$F(q)=\pm\pi+i\frac{\vartheta_4'(v)}{\vartheta_4(v)}=\pm\pi+2iK(k)Z(2K(k)v), \tag{A18}$$

where $v\equiv\beta/2\omega, 0\leqslant v\leqslant 1/2$, and $Z(u)\equiv E(u,k)-uE(k)/K(k)$ is the Jacobi zeta function [24]. Equation (3.12) gives its series expansion. We see that the solution $U_q(\tau)$ decreases with τ. The other independent solution $U_q(-\tau)$ grows with τ.

Notice that $U_q(\tau)$ becomes just an antiperiodic function on the borders of this forbidden band, $v=0$ and $v=1/2$.

It is useful to write the solution $U_q(\tau)$ in terms of Jacobi ϑ functions. Using Eqs. (A6) and (A17) and [19]

$$\sigma(z)=\frac{2\omega}{\vartheta_1'(0)}e^{\eta z^2/2\omega}\vartheta_1\left(\frac{z}{2\omega}\right), \tag{A19}$$

we found Eq. (3.10) after some calculation.

For the allowed band $\eta_0/\sqrt{2}\leqslant q\leqslant\infty$, we find Eq. (3.21) using (A6), Eq. (A17), and Eq. (A19).

2. Broken symmetry case

We derive here the solution of the mode equation (4.5),

$$\left[\frac{d^2}{d\tau^2}+q^2-1+\frac{\eta_0^2}{\mathrm{dn}^2\left(\tau\sqrt{1-\frac{\eta_0^2}{2}},k\right)}\right]\varphi_q(\tau)=0. \tag{A20}$$

It is convenient to express the Jacobi function dn in terms of the Weierstrass $\mathcal{P}$ function through [20]

$$\frac{1}{\mathrm{dn}^2(u,k)}=\frac{1}{e_1-e_2}\left[e_1-\mathcal{P}\left(\frac{u+K(k)+iK'(k)}{\sqrt{e_1-e_3}}\right)\right]. \tag{A21}$$

Where now for convenience and without loss of generality we choose $e_1-e_3=1-\eta_0^2/2$. Then, we find $3e_1=1, 3e_2=1-\frac{3}{2}\eta_0^2$, and $3e_3=\frac{3}{2}\eta_0^2-2$.

Collecting all factors the mode equation (A20) becomes

$$\left[\frac{d^2}{d\tau^2}+q^2-\tfrac{1}{3}-2\,\mathcal{P}(\tau+\omega+\omega')\right]\varphi_q(\tau)=0, \tag{A22}$$

where $\omega'\equiv iK'(k)/\sqrt{1-\eta_0^2}$. This equation is equivalent to Eq. (A5) up to the sign in front of the $\frac{1}{3}$ and a shift $\tau\to\tau+\omega$.

The solution of Eq. (A22) is given by

$$U_q(\tau)=\frac{\sigma(\tau+\omega+\omega'+z)\sigma(\omega'+\omega)}{\sigma(\tau+\omega+\omega')\sigma(\omega'+\omega+z)}e^{-\tau\zeta(z)}. \tag{A23}$$

z and q^2 are now related by

$$\mathcal{P}(z)=+\tfrac{1}{3}-q^2. \tag{A24}$$

We continue to use the normalization (3.5). Changing τ by $-\tau$ in Eq. (A23) provides in general an independent solution of Eq. (A20).

Equation (A24) maps the real q^2 axis into the four sides of the fundamental square in the z plane. This mapping is better seen writing the Weierstrass $\mathcal{P}(z)$ function in terms of Jacobi sn and cn functions [25] in the four cases. That is,

$$z=\beta,\quad 0\leqslant\beta\leqslant\omega,\quad -\infty\leqslant q^2\leqslant 0,$$

$$q^2=\frac{1}{3}-\mathcal{P}(\beta)=\left(1-\frac{\eta_0^2}{2}\right)\frac{\mathrm{cn}^2\left(\beta\sqrt{1-\frac{\eta_0^2}{2}},k\right)}{\mathrm{sn}^2\left(\beta\sqrt{1-\frac{\eta_0^2}{2}},k\right)},$$

$$z=\omega+i\alpha,\quad 0\leqslant\alpha\leqslant\omega'/i,\quad 0\leqslant q^2\leqslant\frac{\eta_0^2}{2},$$

$$q^2=\frac{1}{3}-\mathcal{P}(\omega+i\alpha)=\frac{\eta_0^2}{2}\mathrm{sn}^2\left(\alpha\sqrt{1-\frac{\eta_0^2}{2}},k'\right),$$

$$z=\omega'+\beta,\quad \omega\geqslant\beta\geqslant 0,\quad \frac{\eta_0^2}{2}\leqslant q^2\leqslant 1-\frac{\eta_0^2}{2},$$

$$q^2=\frac{1}{3}-\mathcal{P}(\omega'+\beta)=1-\frac{\eta_0^2}{2}-(1-\eta_0^2)\mathrm{sn}^2\left(\beta\sqrt{1-\frac{\eta_0^2}{2}},k\right),$$

$$z=i\alpha,\quad \omega'/i\geqslant\alpha\geqslant 0,\quad 1-\frac{\eta_0^2}{2}\leqslant q^2\leqslant+\infty,$$

$$q^2=\frac{1}{3}-\mathcal{P}(i\alpha)=\frac{1-\frac{\eta_0^2}{2}}{\mathrm{sn}^2\left(\alpha\sqrt{1-\frac{\eta_0^2}{2}},k'\right)},\qquad \text{(A25)}$$

where $\omega\equiv K(k)/\sqrt{1-\eta_0^2/2}$. Notice that 2ω is the period in τ of the potential in Eqs. (A20) and (A22).

Equation (3.4) holds for the mode function (A23) too. Hence, there are *two* allowed bands

$$z=i\alpha \text{ and } z=i\alpha+\omega, \qquad \text{(A26)}$$

with real $\alpha, 0<\alpha<\omega'/i$, and *two* forbidden bands

$$z=\beta \text{ and } z=\beta+\omega', \qquad \text{(A27)}$$

with real $\beta, 0<\beta<\omega$.

In terms of q^2 the allowed bands correspond to

$$0\leqslant q^2\leqslant\frac{\eta_0^2}{2} \text{ and } 1-\frac{\eta_0^2}{2}\leqslant q^2\leqslant+\infty, \qquad \text{(A28)}$$

and the forbidden bands to

$$-\infty\leqslant q^2\leqslant 0 \text{ and } \frac{\eta_0^2}{2}\leqslant q^2\leqslant 1-\frac{\eta_0^2}{2}. \qquad \text{(A29)}$$

The last forbidden band is for *positive* q^2 and hence *does* contribute to the fluctuation function $\Sigma(\tau)$. $\Sigma(\tau)$ will grow exponentially in time due to the presence of such unstable modes.

It is useful to write the solution $U_q(\tau)$ in terms of Jacobi ϑ functions. For the forbidden band $\eta_0^2/2\leqslant q^2\leqslant 1-\eta_0^2/2$, we obtain Eq. (4.8), using Eqs. (A23), (A17), and (A19), after some calculation.

For the allowed band $1-\eta_0^2/2\leqslant q^2\leqslant+\infty$, we find Eq. (4.11) from Eqs. (A23), (A17), and (A19). The analogous expression (4.13) holds in the allowed band $0\leqslant q^2\leqslant\eta_0^2/2$.

[1] L. Kofman, A. Linde, and A. Starobinsky, Phys. Rev. Lett. **73**, 3195 (1994); **76**, 1011 (1996); in *The Early Universe*, Proceedings of the Chalonge Erice School, NATO ASI Series C: Vol. 467, 1995, edited by N. Sánchez and A. Zichichi (Kluwer Academic, Norwell, MA, 1995); ''Quantum Cosmology and the Structure of Inflationary Universe,'' Report No. gr-qc/9508019, 1995 (unpublished); L. Kofman, Report No. astro-ph/9605155, 1996 [in ''Relativistic Astrophysics: A Conference in Honor of Igor Novikov's 60th Birthday,'' edited by B. Jones and D. Markovic (Cambridge University Press, Cambridge, England, in press)].

[2] Y. Shtanov, J. Traschen, and R. Brandenberger, Phys. Rev. D **51**, 5438 (1995).

[3] D. Boyanovsky, H. J. de Vega, R. Holman, D.-S. Lee, and A. Singh, Phys. Rev. D **51,** 4419 (1995); see, for a review, D. Boyanovsky, H. J. de Vega, and R. Holman, in the *Proceedings of the Second Paris Cosmology Colloquium*, 1994, edited by H. J. de Vega and N. Sánchez (World Scientific, Singapore, 1995), pp. 127–215; D. Boyanovsky, M. D'Attanasio, H. J. de Vega, R. Holman, and D. S. Lee, Phys. Rev. D **52**, 6805 (1995); D. Boyanovsky, M. D'Attanasio, H. J. de Vega, and R. Holman, *ibid.* **54**, 1748 (1996), and references therein.

[4] A. D. Linde, *Particle Physics and Inflationary Cosmology* (Harwood, Chur, Switzerland, 1990).

[5] E. Kolb and M. S. Turner, *The Early Universe* (Addison-Wesley, Redwood City, CA, 1990).

[6] A. D. Dolgov and A. D. Linde, Phys. Lett. **116B**, 329 (1982); L. F. Abbott, E. Farhi, and M. Wise, *ibid.* **117B**, 29 (1982).

[7] S. Mrowczynski and B. Muller, Phys. Lett. B **363**, 1 (1995).

[8] F. Cooper, J. M. Eisenberg, Y. Kluger, E. Mottola, and B. Svetitsky, Phys. Rev. Lett. **67**, 2427 (1991); F. Cooper, in *Particle Production in Highly Excited Matter*, Proceedings of the NATO ASI, edited by H. Gutgrod and J. Rafelski (Plenum, New York, 1993); F. Cooper, J. M. Eisenberg, Y. Kluger, E. Mottola, and B. Svetitsky, Phys. Rev. D **48**, 190 (1993); see also J. M. Eisenberg and Y. Kluger, in *Hot and Dense Nuclear Matter*, edited by W. Greiner, H. Stocker, and A. Gallmann, NATO ASI Series (Plenum, New York, 1994), pp. 333, 635.

[9] F. Cooper and E. Mottola, Mod. Phys. Lett. A **2**, 635 (1987); F. Cooper, S. Habib, Y. Kluger, E. Mottola, J. P. Paz, and P. R. Anderson, Phys. Rev. D **50**, 2848 (1994); F. Cooper, S.-Y. Pi, and P. N. Stancioff, *ibid.* **34**, 3831 (1986); F. Cooper, Y. Kluger, E. Mottola, and J. P. Paz, *ibid.* **51**, 2377 (1995).

[10] S. Habib, Y. Kluger, E. Mottola, and J. P. Paz, Phys. Rev. Lett. **76**, 4660 (1996).

[11] D. Boyanovsky and H. J. de Vega, Phys. Rev. D **47**, 2343 (1993); D. Boyanovsky, H. J. de Vega, and R. Holman, *ibid.* **49**, 2769 (1994).

[12] H. Fujisaki, K. Kumekawa, M. Yamaguchi, and M.Yoshimura, ''Particle Production and Dissipative Cosmic Field,'' Report No. hep-ph-9508378, 1995 (unpublished).

[13] I. I. Tkachev, Phys. Lett. B **376**, 35 (1996); A. Riotto and I. I. Tkachev, ''Non-equilibrium symmetry restoration beyond one loop,'' Report No. hep-ph/9604444, OSU-TA-12/96, 1996 (unpublished); S. Klebnhikov and I. Tkachev, Phys. Rev. Lett. **77**, 219 (1996).

[14] M. Yoshimura, Prog. Theor. Phys. **94**, 873 (1995); ''Baryogenesis and Thermal History after Inflation,'' Report No. hep-ph 9605246 (unpublished).

[15] D. T. Son, Phys. Rev. D **54**, 3745 (1996).

[16] See for a critical discussion, D. Boyanovsky, H. J. de Vega, R. Holman, and J. F. J. Salgado, ''Preheating and Reheating in

Inflationary Cosmology: a pedagogical survey,'' Report No. astro-ph/9609007 [in the Proceedings of the Paris Euronetwork Meeting ''String Gravity'' (unpublished)].

[17] Edward W. Kolb and Antonio Riotto, ''Preheating and symmetry restoration in collisions of vacuum bubbles,'' Report No. astro-ph/9602095, FERMILAB-Pub-96/036-A, 1996 (unpublished).

[18] Edward W. Kolb, Andrei Linde, and Antonio Riotto, ''GUT Baryogenesis after Preheating,'' Report No. hep-ph/9606260, FERMILAB-Pub-96/133-A, SU-ITP-96-22, 1996 (unpublished); Greg W. Anderson, Andrei Linde, and Antonio Riotto, Phys. Rev. Lett. **77**, 3716 (1996).

[19] J. Schwinger, J. Math. Phys. (N.Y.) **2**, 407 (1961); P. M. Bakshi and K. T. Mahanthappa, *ibid.* **4**, 1 (1963); **4**, 12 (1963); L. V. Keldysh, Sov. Phys. JETP **20**, 1018 (1965); A. Niemi and G. Semenoff, Ann. Phys. (N.Y.) **152**, 105 (1984); E. Calzetta, *ibid.* **190**, 32 (1989); R. D. Jordan, Phys. Rev. D **33**, 444 (1986); N. P. Landsman and C. G. van Weert, Phys. Rep. **145**, 141 (1987); R. L. Kobes and K. L. Kowalski, Phys. Rev. D **34**, 513 (1986); R. L. Kobes, G. W. Semenoff, and N. Weiss, Z. Phys. C **29**, 371 (1985).

[20] See, for example, E. Calzetta and B. L. Hu, Phys. Rev. D **35**, 495 (1988); **37**, 2838 (1988); J. P. Paz, *ibid.* **41**, 1054 (1990); **42**, 529 (1990); B. L. Hu, Lectures given at the Canadian Summer School For Theoretical Physics and the Third International Workshop on Thermal Field Theories (Banff, Canada, 1993) (to appear in the proceedings) and in the *Proceedings of the Second Paris Cosmology Colloquium*, 1994, edited by H. J. de Vega and N. Sánchez (World Scientific, Singapore, 1995), p. 111 and references therein.

[21] See, for example, J. Zinn-Justin, *Quantum Field Theory and Critical Phenomena* (Oxford University Press, 1989).

[22] C. Hermite, ''Notes de Cours à l'École Polytechnique,'' 1872 (unpublished); E. T. Whittaker and G. N. Watson, *A Course on Modern Analysis* (AMS, Providence, 1979).

[23] E. L. Ince, *Ordinary Differential Equations* (Dover, New York, 1944).

[24] Bateman Manuscript Project, chapter XIII, Vol. II, edited by A. Erdély (McGraw-Hill, New York, 1953).

[25] I. S. Gradshteyn and I. M. Ryshik, *Tables of Integrals, Series and Products* (Academic, New York, 1980).

[26] A. P. Prudnikov, Yu. A. Brichkov, and O. I. Marichev, *Integrals and Series*, Vol. II (Nauka, Moscow, 1981).

[27] D. Boyanovsky, D.-S. Lee, and I. D. Lawrie, Phys. Rev. D **54**, 4013 (1996).

[28] N. Tetradis, Phys. Lett. B **347**, 120 (1995); N. Tetradis and C. Wetterich, Int. J. Mod. Phys. A **9**, 4029 (1994).

[29] F. Cooper, Y. Kluger, S. Habib, and E. Mottola, ''Symmetry Breaking in Nonequilibrium Mean Field Theory,'' Los Alamos report, 1996 (unpublished).

[30] *Handbook of Mathematical Functions*, edited by M. Abramowitz and I. A. Stegun (NBS, Washington, D.C., 1965).